A CLIMATOLOGY OF NON-CONVECTIVE HIGH WIND EVENTS IN WESTERN NEW YORK STATE

THOMAS A. NIZIOL
THOMAS J. PAONE

National Weather Service Forecast Office
Buffalo, New York

NOAA TECHNICAL MEMORANDA
National Weather Service, Eastern Region Subseries

The National Weather Service Eastern Region (ER) Subseries provides an informal medium for the documentation and quick dissemination of results not appropriate, or not yet ready for formal publications. The series is used to report on work in progress, to describe technical procedures and practices, or to relate progress to a limited audience. These Technical Memoranda will report on investigations devoted primarily to regional and local problems of interest mainly to ER personnel, and usually will not be widely distributed.

Papers 1 to 22 are in the former series, ESSA Technical Memoranda, Eastern Region Technical Memoranda (ERTM); papers 23 to 37 are in the former series, ESSA Technical Memoranda, Weather Bureau Technical Memoranda (WBTM). Beginning with 38, the papers are now part of the series, NOAA Technical Memoranda NWS.

Papers 1 to 22 are available from the National Weather Service Eastern Region, Scientific Services Division, 630 Johnson Avenue, Bohemia, NY, 11716. Beginning with 23, the papers are available from the National Technical Information Service, U.S. Department of Commerce, Sills Bldg., 5285 Port Royal Road, Springfield, VA 22161. Prices vary for paper copy and for microfiche. Order by accession number shown in parentheses at end of each entry.

ESSA Technical Memoranda

ERTM	1	Local Uses of Vorticity Prognoses in Weather Prediction. Carlos R. Dunn. April 1965.
ERTM	2	Application of the Barotropic Vorticity Prognostic Field to the Surface Forecast Problem. Silvio G. Simplicio. July 1965.
ERTM	3	A Technique for Deriving an Objective Precipitation Forecast Scheme for Columbus, Ohio. Robert Kuessner. September 1965.
ERTM	4	Stepwise Procedures for Developing Objective Aids for Forecasting the Probability of Precipitation. Carlos R. Dunn. November 1965.
ERTM	5	A Comparative Verification of 300 mb. Winds and Temperatures Based on NMC Computer Products Before and After Manual Processing. Silvio G. Simplicio. March 1966.
ERTM	6	Evaluation of OFDEV Technical Note No. 17. Richard M. DeAngelis. March 1966.
ERTM	7	Verification of Probability of Forecasts at Hartford, Connecticut, for the Period 1963-1965. Robert B. Wassall. March 1966.
ERTM	8	Forest-Fire Pollution Episode in West Virginia, November 8-12, 1964. Robert O. Weedfall. April 1966.
ERTM	9	The Utilization of Radar in Meso-Scale Synoptic Analysis and Forecasting. Jerry D. Hill. March 1966.
ERTM	10	Preliminary Evaluation of Probability of Precipitation Experiment. Carlos R. Dunn. May 1966.
ERTM	11	Final Report. A Comparative Verification of 300 mb. Winds and Temperatures Based on NMC Computer Products Before and After Manual Processing. Silvio G.Simplicio. May 1966.
ERTM	12	Summary of Scientific Services Division Development Work in Sub-Synoptic Scale Analysis and Prediction - Fiscal Year 1966. Fred L. Zuckerberg. May 1966.
ERTM	13	A Survey of the Role of Non-Adiabatic Heating and Cooling in Relation of the Development of Mid-Latitude Synoptic Systems. Constantine Zois. July 1966.
ERTM	14	The Forecasting of Extratropical Onshore Gales at the Virginia Capes. Glen V. Sachse. August 1966.
ERTM	15	Solar Radiation and Clover Temperatures. Alex J. Kish. September 1966.
ERTM	16	The Effects of Dams, Reservoirs and Levees on River Forecasting. Richard M. Greening. September 1966.
ERTM	17	Use of Reflectivity Measurements and Reflectivity Profiles for Determining Severe Storms. Robert E. Hamilton. October 1966.
ERTM	18	Procedure for Developing a Nomograph for Use in Forecasting Phenological Events from Growing Degree Days. John C. Purvis and Milton Brown. December 1966.
ERTM	19	Snowfall Statistics for Williamsport, Pa. Jack Hummel. January 1967
ERTM	20	Forecasting Maturity Date of Snap Beans in South Carolina. Alex J. Kish. March 1967.
ERTM	21	New England Coastal Fog. Richard Fay. April 1967.
ERTM	22	Rainfall Probability at Five Stations Near Pickens, South Carolina, 1957-1963. John C. Purvis. April 1967.
WBTM ER	23	A Study of the Effect of Sea Surface Temperature on the Areal Distribution of Radar Detected Precipitation Over the South Carolina Coastal Waters. Edward Paquet. June 1967. (PB-180-612).
WBTM ER	24	An Example of Radar as a Tool in Forecasting Tidal Flooding. Edward P. Johnson. August 1967 (PB-180-613).
WBTM ER	25	Average Mixing Depths and Transport Wind Speeds over Eastern United States in 1965. Marvin E. Miller. August 1967. (PB-180-614).
WBTM ER	26	The Sleet Bright Band. Donald Marier. October 1967. (PB-180-615).
WBTM ER	27	A Study of Areas of Maximum Echo Tops in the Washington, D.C. Area During the Spring and Fall Months. Marie D. Fellechner. April 1968. (PB-179-339).
WBTM ER	28	Washington Metropolitan Area Precipitation and Temperature Patterns. C.A. Woollum and N.L. Canfield. June 1968. (PB-179-340).
WBTM ER	29	Climatological Regime of Rainfall Associated with Hurricanes after Landfall. Robert W. Schoner. June 1968. (PB-179-341).
WBTM ER	30	Monthly Precipitation - Amount Probabilities for Selected Stations in Virginia. M.H. Bailey. June 1968. (PB-179-342).
WBTM ER	31	A Study of the Areal Distribution of Radar Detected Precipitation at Charleston, S.C. S.K. Parrish and M.A. Lopez. October 1968. (PB-180-480).
WBTM ER	32	The Meteorological and Hydrological Aspects of the May 1968 New Jersey Floods. Albert S. Kachic and William Long. February 1969. (Revised July 1970). (PB-194-222).
WBTM ER	33	A Climatology of Weather that Affects Prescribed Burning Operations at Columbia, South Carolina. S.E. Wasserman and J.D. Kanupp. December 1968. (COM-71-00194).
WBTM ER	34	A Review of Use of Radar in Detection of Tornadoes and Hail. R.E. Hamilton. December 1969. (PB-188-315).
WBTM ER	35	Objective Forecasts of Precipitation Using PE Model Output. Stanley E. Wasserman. July 1970. (PB-193-378).
WBTM ER	36	Summary of Radar Echoes in 1967 Near Buffalo, N.Y. Richard K. Sheffield. September 1970. (COM-71-00310).
WBTM ER	37	Objective Mesoscale Temperature Forecasts. Joseph P. Sobel. September 1970. (COM-71-0074).

NOAA Technical Memoranda NWS

NWS	ER 38	Use of Primitive Equation Model Output to Forecast Winter Precipitation in the Northeast Coastal Sections of the United States. Stanley E. Wasserman and Harvey Rosenblum. December 1970. (COM-71-00138).
NWS	ER 39	A Preliminary Climatology of Air Quality in Ohio. Marvin E. Miller. January 1971. (COM-71-00204).
NWS	ER 40	Use of Detailed Radar Intensity Data in Mesoscale Surface Analysis. Robert E. Hamilton. March 1971. (COM-71-00573).
NWS	ER 41	A Relationship Between Snow Accumulation and Snow Intensity as Determined from Visibility. Stanley E. Wasserman and Daniel J. Monte. (COM-71-00763). January 1971.
NWS	ER 42	A Case Study of Radar Determined Rainfall as Compared to Rain Gage Measurements. Martin Ross. July 1971. (COM-71-00897).
NWS	ER 43	Snow Squalls in the Lee of Lake Erie and Lake Ontario. Jerry D. Hill. August 1971. (COM-72-00959).
NWS	ER 44	Forecasting Precipitation Type at Greer, South Carolina. John C. Purvis. December 1971. (COM-72-10332).
NWS	ER 45	Forecasting Type of Precipitation. Stanley E. Wasserman. January 1972. (COM-72-10316).

NOAA Technical Memorandum NWS ER-91

A CLIMATOLOGY OF NON-CONVECTIVE HIGH WIND EVENTS IN WESTERN NEW YORK STATE

THOMAS A. NIZIOL
THOMAS J. PAONE

National Weather Service Forecast Office
Buffalo, New York

TABLE OF CONTENTS

ABSTRACT

Strong winds are common to the Great Lakes region, western New York in particular, and are responsible for significant damage and monetary loss each year. Although damage often occurs from thunderstorm or convectively induced wind gusts, numerous non-convective high wind events occur with the passage of strong synoptic scale weather systems across the area.

A total of 52 non-convective high wind events over a 20-year period were identified and analyzed in western New York. Various results were calculated from the data including the seasonality of the occurrence of high wind episodes and the prevailing wind direction for each event. Tracks of the surface lows were plotted by month and composite atmospheric fields of sea level pressure, 850 mb height and temperature and 500 mb heights were constructed to provide the synoptic scale pattern conducive to such events. Select case studies were also analyzed to identify additional parameters conducive to non-convective high wind events that are not possible to evaluate from a climatological point of view.

The occurrence of high wind events showed a marked seasonality from late Fall through early Spring. The prevailing wind direction was predominantly southwest to west with relatively few events occurring from a northwest through southeast direction. Tracks of surface lows were similar, with the centers moving from southwest to northeast and passing generally to the north and west of the area of study. Composite atmospheric fields revealed a particular synoptic scale weather pattern conducive to high wind events across western New York. Case studies highlighted other significant parameters conducive to the development of high winds that are not apparent in the climatological composite charts. The information presented here will hopefully provide forecasters with a better understanding of these events.

1. INTRODUCTION

High winds produce significant damage and monetary loss across the Great Lakes Region and western New York each year. Damage is not restricted to inland areas but ravages lakeshore areas too. A windstorm that occurred at the east end of Lake Erie on 1-2 December 1985 produced millions of dollars of losses on both the American and Canadian shores. Hundreds of homes were damaged along with the loss of substantial amounts of lakefront property (Storm Data 1985). In fact, from a historical point of view, the loss of life attributed to such storms on the Great Lakes during 1868-69 prompted the United States Congress to form a national weather service (Hughes 1970).

Non-convective high wind events generally occur in association with strong cyclones that cross the Great Lakes Region. Angel and Isard (1998) reviewed the frequency and intensity of Great Lakes cyclones and found that the frequency of strong cyclones was greatest during the cold season months from November through April. Kapela et al. (1995) studied wintertime post cold frontal wind events over the Northern Plains. They identified several atmospheric ingredients that contribute to high winds. From their list of parameters an operational checklist was developed to assist the forecaster in the issuance of high wind warnings. Lee and Girodo (1999) analyzed low-level lapse rates to detect the depth of the mixed layer and subsequent potential for the downward mixing of strong winds to the surface. They found that the ability to determine the depth of the mixed layer is very important to the prediction of surface wind speed.

This study was motivated by a need to develop a climatology of high wind events across western New York to be used as a guidance tool for operational forecasters. The seasonality of such events was determined to highlight the most critical time of occurrence throughout the year. Events were also stratified by wind direction. To learn the common synoptic scale patterns that produce such events composite atmospheric fields of sea level pressure, 850 mb height and temperature and 500 mb heights were constructed from the data. Atmospheric soundings were also analyzed for each event to detect specific patterns of temperature, moisture and wind profiles. Finally, the last section of the paper presents two case studies to highlight features shown to be common to such storms in other parts of the country (Kapela et al. 1995). In particular, the surface isallobaric pattern associated with the storms will be compared to processes that are ongoing farther up in the atmosphere. The case studies will reinforce the importance of hourly surface analyses that can indirectly provide valuable information on processes at that may be ongoing at other levels in the atmosphere.

2. DATA

To get some perspective on just how windy western New York is, 140 U.S. cities were ranked for average wind speed during the winter months (National Climatic Data Center 1993). Buffalo, New York, located at the eastern end of Lake Erie was ranked as the tenth windiest city in the U.S. during the winter season (Table 1). Other eastern Great Lakes locales ranked relatively high on the list included Erie, Pennsylvania at 23rd and Cleveland, Ohio at 33rd. For this study, Buffalo was chosen as the representative site for data analysis in western New York.

A high wind event was defined as a day in which a non-convective thunderstorm wind gust of 50 knots or greater was recorded at Buffalo, New York. Those events identified as a result of

thunderstorm wind gusts were eliminated from the data set. The study period comprised a data set that spanned a twenty-year period from 1977 through 1997. Events were chosen from locally archived data at the National Weather Service office at Buffalo, NY. For each high wind event identified, atmospheric composites of sea level pressure, 850 mb height and temperature, and 500 mb heights were calculated. This information was obtained from the National Center for Environmental Prediction (NCEP) octogonal grids (Jenne 1975). In addition, for each event, archived atmospheric soundings taken at Buffalo, NY were analyzed. The sounding data was compiled from the National Climatic Data Center (NCDC 1995).

3. RESULTS

High wind events were categorized by each month of the year (Figure 2). They showed a preponderance for occurrence during the late Fall through early Spring, corresponding closely with Angel and Isard's (1998) frequency of Great Lakes cyclones, which were most prevalent during the cold season months from October through April. The data also matches very well with the work described by Pore et al.(1975) describing the climatology of Lake Erie storm surges at Buffalo, NY. In their study it was determined that 94% of significant storm surges at Buffalo occurred during the period from September through April.

The events were also categorized by wind direction and the results were even more dramatic. An overwhelming number of events occurred with wind direction from southwest or west (Figure 3). Virtually no events occurred with winds directions from north through southeast. The results suggest that there may be other factors that could have led to such an overwhelming percentage of southwest to west winds. Buffalo's location on Lake Erie may play an important role in the stratification of wind direction. Buffalo is located immediately downwind of the long fetch of the elliptically shaped lake. Lake Erie narrows significantly at its eastern end and produces increased channeling of southwest to west winds at Buffalo. Richards (1966) also showed that in cases when cold air overrides the warmer lake waters, common during the fall through winter months, one can expect a significant increase in wind speed. It would seem reasonable therefore that Buffalo and the western New York area would see most of their high wind events occur during the cold seasons of the year with prevailing winds from a southwest to west direction.

The track of the associated surface lows that eventually produced high winds were plotted on a monthly basis. In general, storm tracks do show a definite and expected pattern, with surface lows moving from southwest to northeast and passing to the north and west of the eastern Great Lakes region, though there were a few exceptions, mainly during the month of January (Figures 4a-g). The storm tracks match very well with the observation that all of the high wind events occurred in the southwest to west quadrant of the surface low in the wake of the cold frontal passage.

To develop a more thorough understanding of the synoptic scale pattern that produces non-convective high winds, a series of composite atmospheric charts were constructed by averaging each parameter over the 52 cases. The charts included sea level pressure, 850 mb height and temperature, and 500 mb height, temperature and vorticity. The composites, available at 12-hr intervals and shown in Figures 5-7, were plotted for approximately twelve hours before the high wind event occurred (t-12h), near the time of occurrence of the high wind event (t=0h), and twelve hours after

2

the event occurred (t+12h). The composites do not provide in-depth analyses of the forcing functions or other atmospheric parameters responsible for high wind events. However, they do point out to the operational forecaster the general synoptic scale pattern conducive to such events.

The 500 mb height fields (Figure 5a-5c) revealed a meridional trough at t-12h over the center of the U.S. The axis of the trough swings through the eastern Great Lakes between t=0h and t+12h. The associated vorticity field indicates a vorticity maximum that tracks from southwest to northeast across the Great Lakes region during the period of high winds. This scenario generally is in accordance with the evidence provided by Kapela et al. (1995) on Northern Plains events except in the current study the vorticity center moves in a northeast direction as compared to their southeast moving feature. However, the result is similar, namely the eastern Great Lakes region is under an area of strong anticyclonic vorticity advection (AVA) and related subsidence and downward momentum transfer aloft during the period that high winds were recorded (Saucier, 1955)

The composite 850 mb height and temperature advection fields (Figure 6a-c) indicate a closed low at t-12h that moves eastward, just to the north and west of the eastern Great Lakes. This pattern shows a tightly packed height field to the south of the center of the low and certainly suggests a strong southwest to west wind field across the eastern Great Lakes. The associated temperature advection field clearly indicates a well defined temperature rise/fall couplet that crosses the eastern Great Lakes region. Significant cold air advection is taking place at this level during the period of strong winds. Strong cold air advection through the lower levels of the atmosphere ensures steep lapse rates that are necessary to produce downward transport of higher momentum air to the surface.

Finally, MSLP composites (Figure 7a-c) clearly show a strong closed low that deepens as it moves in a northeast direction to the north and west of the eastern Great Lakes. During the time of strongest winds (t=0h) the composite suggests that cold frontal passage has occurred with a very tightly packed pressure gradient across the eastern Great Lakes producing strong southwest to west winds over the region.

Although the composite charts provide an excellent description of the major synoptic scale features that produce such high wind events, there are other parameters that are very important in the prediction of high winds. One scenario that forecasters often face in western New York occurs ahead of cold fronts. In such a pattern there is often a lack of strong surface winds when the winds aloft are very strong. Wind speeds at 850 mb may be in excess of 50 knots but the downward transport of those high winds does not occur due to a lack of mixing. The lack of mixing is often the result of a small lapse rate or even a temperature inversion.

In an effort to try to quantify this scenario, atmospheric soundings for the high events were compared to a set of soundings described as "decoupled" non-high wind events. The "decoupled" events were compiled for the same time period and were defined when winds greater than 50 knots occurred at 850 mb but were less than 25 knots at the surface. As Table 2 indicates, the average surface to 850 mb lapse rate for high wind events was approximately 8 ° C, but for non-events the lapse rates were only about 3.5 ° C. In addition, there was significant veering in the wind direction from the surface through 850 mb in non-events, suggesting strong warm air advection, whereas in the high wind events, winds were almost unidirectional through that layer.

It is very important therefore to not only understand the synoptic scale pattern that is conducive to these events but to look at other features as well. Two case studies of high wind events in western New York were analyzed to highlight other forecast parameters that are important predictors for high winds.

4. CASE STUDIES

In the preceding climatological review, it was noted that most of the high wind events that occur in western New York are associated with surface and 850 mb low height centers that move north and west of the area. The 700 mb and 500 mb troughs also followed a southwest to northeast path that tracked just north of the lower Great Lakes. The track of the surface and upper level lows places western New York in a location that favors southwest to west flow during high wind events.

The climatological summary was very helpful in identifying the large-scale synoptic patterns that are associated with high wind events in western New York. It would be worthwhile to go one step further and examine how the synoptic patterns produce temperature profiles and vertical motions that are conducive to high winds at the surface. While this type of analysis is beyond the scope of a climatological study, it is important to examine some of the specific processes that lead to high winds in order to understand the significance of the general climatological trends.

In an investigation of post-cold front high wind events on the northern plains, Kapela et al. (1995) constructed an operational checklist of some of the key factors that are associated with high winds. In this part of the study, we will evaluate several components of this checklist to see how they contributed to two high winds events that affected western New York.

In February 1997, two significant wind storms affected western New York within a time span of one week. In each event, strong low pressure centers moved across southern Ontario and western New York state and were accompanied by a significant change in temperature. The rapid exchange of contrasting air masses produced significant changes in surface pressure which ultimately led to the high winds.

We chose to approach this part of our study from the point of view of a forecaster in a real-time operational setting. High wind events were analyzed using PCGRIDDS and the Eta model. Not only did this allow us to test the effectiveness of Kapela's high wind check list for western New York, we were also able to simulate the steps that a forecaster might have to take to predict high winds.

4.1. 22 February 1997

The first high wind event occurred on 22 February 1997. A strong cold front moved through Buffalo around 0800 UTC, dropping the surface temperature dropped from 15 ° C to 4 ° C in just three hours. Gusty southwest winds preceded the front, but the strongest winds developed after 1200 UTC. This windstorm was significant in both its intensity and duration. A peak wind gust of 56 knots occurred at the Buffalo International airport at 1400 UTC and sustained winds of 30 knots or greater were recorded from 1900 UTC through 2400 UTC. In addition, wind gusts of 30 knots or

higher were recorded for almost twelve hours. The high winds had a substantial effect on western New York. In Buffalo and Rochester, the combined structural damage totalled over one million dollars and flooding occurred along the east end of Lake Erie (Storm Data 1997).

4.1a. Cold Air Advection

The Eta model, initialized at 0000 UTC 22 February 1997, showed a 994 mb surface low located in the vicinity of southern Michigan and northern Ohio. Between 0600 UTC and 1200 UTC, the surface low was forecast to move from Buffalo to Watertown before reaching the New England states by 1800 UTC (Fig 8a-c). The forecast track of the 850 mb low followed a similar path except that is was farther to the north and west (Fig 8d-f). The 700 mb low was displaced even farther to the northwest, in the direction of the colder air. This is a pattern that would be expected with a well developed extra-tropical low.

The onset of the cold air advection over western New York was accompanied by a lowering of the 1000-500 mb thickness values shortly after 0600 UTC. At 850 mb, the closely spaced height lines crossed the isotherms at nearly right angles, implying strong cold air advection at this level as well (Figures 8d-f).

Following the example of Kapela et al. (1995) , the cold air advection pattern was analyzed through the 850-500 mb layer. The Eta 1000-500 mb thickness field and the temperature advection at 850mb suggested that the cold air advection would last from about 0600 UTC until 1800 UTC. During this period, the thickness values near Buffalo lowered from 553 dm to 528 dm. The Eta also forecast a corresponding temperature decrease of 26 ° C at 850 mb, 22 ° C at 700 mb and 20 ° C at 500 mb. It is noteworthy that the strongest cold air advection was forecast to occur in the lower levels. This is often the case during cold air outbreaks. The strong subsidence (and resulting adiabatic warming), that is commonly associated with very cold air, works to slow down the cold air advection at the middle and upper levels of the atmosphere. This may have important implications which will be addressed later. To summarize up to this point, the Eta model indicated a very tight surface pressure gradient and strong cold air advection through a deep layer. Forecasters know from their experience that a tight surface pressure gradient does not always guarantee that high winds will develop at the surface. Sometimes, in the warm sector ahead of cold fronts, strong winds are observed at 850 mb. However, the presence of a temperature inversion ahead of the front will inhibit mixing and prevent the transport of higher winds aloft down to the surface.

The main point to emphasize is that the presence of a deep layer of very cold air does indicate a potential for strong subsidence which can lead to the transfer of high momentum air down to the lower levels of the atmosphere.

4.1b. Subsidence

With a deep layer of cold air in place after 0600 UTC on the 22nd, we must consider if there is a mechanism that will help to transport cold, high momentum air down to the surface. In Figure 9a-c, the 1000-500 mb thickness field overlaps the vorticity isopleths at 500 mb. Combining the thermal advection through the 1000-500 mb layer, with the vorticity advection at 500 mb is one way we can

apply the omega equation to determine where upward motion or subsidence will be occurring in the atmosphere.

While it is more accurate to relate vertical motions to differential vorticity advection through a layer of the atmosphere, many forecasters examine the vorticity at 500 mb to get a first approximation where large scale upward motion (or subsidence) is likely to occur. Since the level of nondivergerce is close to 500 mb, this approximation often works fairly well. In an attempt to identify regions of strong subsidence in the atmosphere, Kapela et al. focused on areas that were upstream of upper level troughs. Specifically, they looked for areas where tightly packed vorticity isopleths overlapped tightly packed thickness line (often referred to as Negative Isothermal Vorticity Advection or NIVA) that were decreasing in value. Applying the omega equation, we can reason that a combination of strong anticyclonic vorticity advection (AVA) and strong cold air advection imply sinking motion (Bluestein,1992).

Figure 9a (0600 UTC thickness/vorticity) shows weak cyclonic vorticity advection (CVA) over western New York, but the strongest AVA and greatest thickness packing is still well to the west. At 1200 UTC (Figure 9b) the Eta showed lower thicknesses over western New York, but CVA is still dominating the target area. Therefore, as of 1200 UTC, these two components of vertical motion are still working against each other and we would not expect to see strong sinking motion through a deep layer in the atmosphere. Looking ahead to 1800 UTC (Figure 9c), the 500 mb trough has moved east of Buffalo and the area of strong AVA is coincident with the tight gradient of lowering thickness values. This implies a potential for strong subsidence between 1200 UTC and 1800 UTC.

Now that we have a mechanism to bring the cold air down, the next question is will the subsiding air work its way all the way down to the surface and generate strong winds? To answer this question, we must look at the Buffalo sounding and examine the lapse rates.

4.1c Lapse Rates

Kapela et al.(1995) remind us that low level cold air advection alone will not sustain strong winds for long a time unless higher momentum air is transported down into the boundary layer. The presence of a steep lapse rate in a well-mixed layer is one to way to accomplish this momentum transfer.

Figure 10a is a reproduction of the 1200 UTC February 22 Buffalo sounding. One obvious feature of the temperature plot is the presence of an inversion from 900 mb to 800 mb. The wind profile shows very strong (greater than 50 knots) southwest winds above 2000 feet AGL. While the surface winds were gusting up to 38 knots at the time the sounding was taken, the stronger winds above 2000 feet had not mixed down to the surface.

The presence of the low level temperature inversion and the noticeable speed shear between 1000 and 2000 feet are clear indications that the sounding is not well mixed at 1200 UTC. Even though this sounding represents conditions four hours after the cold front moved through Buffalo, it appears that the cold air had not filtered down through a deep enough layer to eliminate the inversion. This resulted in a significant difference in the rate of cooling within the boundary layer.

Cold air outbreaks are usually accompanied by strong subsidence which causes the air to warm dry adiabatically. While adiabatic warming of the subsiding air does promote the downward transfer of higher momentum air, this process can be counter-productive to momentum transfer if the lowest layer of the atmosphere cools too quickly. Indeed, this appears to be the case at 1200 UTC. A comparison of the 0000 UTC and 1200 UTC soundings (Figures 10a-b) shows that by 1200 UTC there was a much greater drop in temperature in the region below 900 mb compared to the layers aloft. This resulted in the formation of a temperature inversion which in turn delayed the transfer of stronger winds to the surface by 1200 UTC. The disparity in the rate of cooling within the boundary layer is a good demonstration of Kapela's observation that the processes that support the production of a steep lapse rate must stay one step ahead of the processes that favor the formation of a temperature inversion.

Between 1200 UTC and 1800 UTC, the thermal structure of the atmosphere became much more favorable for the downward transport of the higher momentum air. The Eta's indication of a tight gradient of lowering thickness values and AVA at 500 mb (NIVA) implies strong sinking motion across western New York. A review of the 0000 UTC 23 February Buffalo sounding (Figure 10c) showed that the low level temperature inversion was wiped out and replaced by a superadiabatic lapse rate that extended from the surface up to about 925 mb. Once the inversion was broken, it did not take long for the strong winds to reach the surface. Recall that the strongest winds in Buffalo were observed around 1400 UTC. The main point to emphasize here is that a steep lapse rate is the mechanism that promotes good mixing and allows the higher momentum air to reach the surface.

The 0000 UTC February 23 sounding displays another characteristic that contributes to the transfer of stronger winds to the surface. The wind profile shows less than 30 degrees of directional shear from the surface to 500 mb. The alignment of the winds also makes it possible for better transport of the higher momentum air to the surface (Kapela et al. 1995).

4.1d Surface Pressure Rises

With a steep lapse rate to facilitate the transport of strong winds down to the surface, one would expect to see a significant rise in surface pressure. In an operational setting, a forecaster can monitor the 3-hour pressure changes to identify areas of significant pressure falls or rises. A significant (greater than 3 mb) rise in surface pressure in three hours can alert the forecaster to the possibility of strong winds in the near future (less than six hours). The benefit to the public would be even greater if the forecaster could provide a longer lead in time by issuing a high wind watch. Fortunately, we have another tool in our forecasting arsenal that will help to accomplish this. An isallobaric analysis of model data will help us anticipate the possibility of high winds twelve to twenty-four hours in advance.

To quickly review, the isallobaric component of the horizontal wind is proportional to the time rate of change of the acceleration that is induced by the pressure gradient force (Bluestein 1992). In other words, the isallobaric component of the wind represents an acceleration from an area of pressure rises into an area of pressure falls. The greater the difference between the rise-fall couplet, the stronger the acceleration into the area of pressure falls.

Since we are interested mainly in highs winds that follow the passage of strong cold fronts, it would be beneficial to be able to forecast the track of the isallobaric rise maximums. The 6-hour isallobaric rise-fall couplets from the Eta model during an 18-hour time period are shown in Figures 9d-f. The 0600-1200 UTC rise-fall couplet showed an 11 mb maximum pressure rise over western Ohio, while a much weaker pressure fall maximum was forecast over Quebec province. While this rise-fall couplet spans the time of the cold frontal passage (0900 UTC), the acceleration from the maximum pressure rises into the maximum pressure falls is directed into southern Ontario. This suggests that between 0600 UTC and 1200 UTC the strongest winds would occur over northern Ohio and southeast Michigan and maybe part of Southern Ontario, just east of Lake Huron.

Between 1200 UTC and 1800 UTC , the Eta model showed an isollabaric rise maximum of 14 mb directly over Buffalo. A tight isallobaric gradient stretched across central and northern New York and continued toward the area of maximum low pressure falls, located just north of the New England states. In the time interval from 1800 UTC to 0000 UTC, the isallobaric rise maximum was forecast to move to northern New York state, just east of Watertown. If we follow the track of the isallobaric rise maximum, we can see that the timing of the location of the maximum pressure rises corresponds very closely to the time when the strongest winds were observed in Buffalo (Table 3). That is, the projected path of the isallobaric rise maximum suggested that the strongest winds in western New York would occur in the time interval from a little after 1200 UTC to about 2100 UTC. During the time period when the strongest pressure rises and tight isallobaric gradient were forecast to move east of Buffalo, the surface observations showed a corresponding decrease in wind speed. From Table 3 we can also compute the 3-hour pressure rises at the surface and see how these relate to the peak winds that were observed during each 3-hour time interval. The trend of the plot of the 3-hour pressure rises is what you would expect when high momentum air aloft is transported down to the surface.

It is important to note that while most of western and central New York experienced high winds as the surface low moved across Lake Ontario, the strongest winds were felt downwind of Lake Erie from Buffalo to Rochester. This is consistent with climatology. Also recall that the shape and east-west orientation of Lake Erie creates a channeling affect that enhances the southwest to west winds in Buffalo and areas downwind of the lake.

To briefly summarize, on 22 February 1997 a tight pressure gradient around a well- developed low hinted at the possibility of strong winds across western and central New York.   The combination of strong cold air advection through a deep layer of the atmosphere and strong AVA at 500 mb suggested good potential for subsidence. Finally, the presence of a steep lapse rate promoted good mixing which ultimately encouraged the transfer of strong winds down to the surface. The strong surface winds were accompanied by 3-hourly pressure rises that ranged from 6 mb to 10 mb. The strong winds and surface pressure rises also correlated very well with the forecast track of an area maximum isallobaric rises.

Since all the factors that lead to strong subsidence in the atmosphere are ultimately reflected in strong pressure rises at the surface, the 3-hour pressure tendency changes become an invaluable tool to predict the location and timing of high winds. This is especially true in an operational setting where there is not always enough time to do a detailed analysis of the model data, or a pertinent sounding may not be available. The forecaster must remain alert to the possibility that high winds

may reach his/her area before the strongest pressure rises are revealed by the 3-hour pressure tendencies on the surface map. Therefore, if high winds are expected within the next 6 hours, for example, it may be a good idea to monitor the pressure changes each hour.

If two consecutive runs of the model data show strong isallobaric rises at the surface, this would certainly give forecasters more confidence in issuing a high wind watch or warning for their area of responsibility. The main point that we wish to make is that performing an isallobaric analysis using the model data is an excellent way to prepare for the possibility of high winds. If the models suggest that there is a good potential for high winds, the forecaster should monitor the upstream observations for strong pressure rises at the surface. The track of the pressure rise/fall couplet at the surface can then be used to identify the general location of the highest winds in the near future.

4.2. 27 February 1997

The second high wind event took place on 27 February 1997 and showed many similarities to the one that affected Buffalo on February 22. A strong low pressure center moved from Indiana to southern Ontario. A cold front that was associated with the low moved through Buffalo around 1700 UTC and was accompanied by an 11 $^\circ$ C drop in temperature in just one hour. The combination of strong cold air advection and rapid pressure rises behind the frontal passage led to very strong southwest winds during the afternoon into the early evening. At 2100 UTC, a peak wind gust of 61 knots was reported at the Buffalo airport and winds gusts of 50 knots or greater were recorded for five consecutive hours. Other wind gusts included 70 knots at Niagara Falls, 65 knots at Rochester and 50 knots at Batavia. These strong winds caused more structural damage across western New York and disrupted air traffic at the Buffalo airport for several hours.

4.2a. Synoptic Pattern and Cold Air Advection

Figure 11 shows the Eta's forecast (initialized at 1200 UTC 27 February) track of the surface and 850 mb low pressure heights. The surface low was forecast to move just north of Buffalo, while the 850 mb low was forecast to follow a path that would take it north of Lake Ontario. These tracks are very similar to the ones taken by the surface and 850 mb composites that were constructed from the climatological study. Isopleths of 850 mb height contours show a very tight west to southwest gradient across Lake Erie and western New York from 1800 UTC through 0000 UTC.

From an analysis of the model thickness fields and temperature advections at 850 mb, it was determined that cold air advection would begin around 1800 UTC and continue through 0000 UTC. During this time period the Eta indicated a modest temperature decrease of 13 $^\circ$ C at 850 mb, 6 $^\circ$ C at 700 mb and 5 $^\circ$ C at 500 mb, relatively weak cold air advection compared to temperatures changes that were forecast for the February 22 high wind event.

4.2b. Subsidence

At 500 mb, a weak shortwave was forecast to move from the Central Plains and approach western New York shortly after 1800 UTC . Between 1200 UTC and 1800 UTC, the thickness and vorticity patterns (Figures 12a-c) indicated that the Eastern Great Lakes area would be dominated by PIVA. Therefore, no organized subsidence should be expected during this time period. By 0000 UTC 28

February, the Eta showed lowering thickness values and weak AVA (hence NIVA) over western New York. While NIVA does not appear to be as well defined as it was on February 22, the pattern is consistent with Kapela's observation that the strongest subsidence occurs in the west or southwest quadrant of the vorticity center.

4.2c. Lapse Rates

The 1200 UCT 27 February Buffalo sounding (Figure 13) shows an inversion at the surface and another shallow inversion based just below 900 mb. The wind profile shows sharply veering and relatively weak winds in the lowest 5000 feet of the atmosphere. This is a clear indication that warm air advection was occurring at 1200 UTC and we would not expect subsidence to develop. However, above 6000 feet, the wind profile shows a significant increase in wind speed with much less directional shear. This observation is a clue that high winds may develop at the surface later in the day. Unfortunately we cannot analyze the 0000 UTC 28 February Buffalo sounding to see how the lapse rates and wind profiles changed. The strong winds that developed during the afternoon made it impossible to launch an evening sounding. However, we can still do an isallobaric analysis to see if the pressure rise patterns hinted at the possibility of high momentum air being transferred down to the surface.

4.2d. Pressure Changes

Figures 12d-f show the isallobaric fall/rise couplets that the Eta indicated before, during and after the high wind event. Between 1200 UTC and 1800 UTC the model indicated an 18 mb pressure difference between a strong pressure rise center over Indiana and a moderately strong pressure fall center over central New York. The isallobaric gradient was directed toward western New York during this time interval, but the model was still showing pressure falls across the area. During the next 6 hour interval, the Eta indicated a 15 mb pressure rise center over Michigan while the pressure fall center showed a weakening trend as it moved toward the New England states. Finally, between 0000 UTC and 0600 UTC (February 28), the maximum pressure rise was centered just north of Lake Ontario. When we follow the path taken by the isallobaric rise maximum and compare it to the timing of the strongest observed wind speeds in Buffalo (Table 4), it is apparent that the strongest winds occurred during the time period when the Eta had indicated the largest pressure rises across western New York.

4.2e. Implications of the Dry Slot

Kapela et al. (1995) pointed out that the presence of a dry slot in the southwest or western quadrant of a vorticity maximum is another indication that subsidence is occurring in the atmosphere. A comparison of the vorticity pattern with the Eta model indication of mean relative humidity in the 1000-500 mb layer (Figure 14) reveals that on February 27 a well defined dry slot was forecast to develop in the southwest quadrant of the eastward moving vorticity maximum. The heavy arrow on the mean relative humidity plot marks the location of the dry slot. Following the track of the arrow, the model indicated that the dry slot would be in the vicinity of western New York from 1800 UTC through 0000 UTC. Not surprisingly, the location of the dry slot corresponds to the timing of the maximum pressure rises and peak winds across western New York.

A quick review of the surface observations for February 27 (Table 4) shows that from 1900 UTC until 2100 UTC mostly sunny skies were reported at the Buffalo International Airport. This observation is a good indication that a dry slot did indeed work its way into western New York. Since the dry slot is evidence that subsidence is occurring in the atmosphere, we can infer that the

sinking motion and mixing within the dry slot encouraged the downward transfer of strong winds to the surface.

In conclusion, even though the Eta did not indicate strong cold air advection through a deep layer of the atmosphere on February 27, it still hinted at the possibility of strong subsidence in the isallobaric rise pattern and in the development of the dry slot. Without the 0000 UTC sounding, we cannot verify if good mixing within the boundary layer was the mechanism that ultimately transported the high momentum air down to the surface. But, the surface observations did show strong cold air advection and strong pressure rises. The Eta also hinted at the possibility of strong winds in the surface pressure pattern and in the tight height gradient at 850 mb. Finally, the channeling of the winds at the eastern end of Lake Erie undoubtedly made a strong contribution to the increased wind speeds that were observed in Buffalo, Niagara Falls and Rochester.

5. CONCLUDING REMARKS

In general, non-convective high wind events in western New York follow a specific seasonality, occurring from late Fall through the early Spring months. Wind direction is almost always from southwest to west, which coincidentally is the prevailing wind direction in western New York. The orientation of Lake Erie most likely plays an important role in the overwhelming number of high wind events that occur from a southwest to west direction.

High wind events occur under a specific synoptic scale conditions. Storm tracks generally align from southwest to northeast and low centers almost always cross to the north and west of western New York. Composite synoptic scale charts developed from 52 events over a period of 20 years reveal that the surface low generally tracks across the Great Lakes region with tightly packed isobars oriented in a west-east direction, allowing for strong southwest surface winds to develop across western New York. The structure of the low is tilted slightly toward the northwest and colder air. At 850 mb, a closed low tracks from the western Great Lakes, northeast through the province of Ontario just south of James Bay, Canada. The low is accompanied by a temperature rise/fall couplet that produces very strong cold air advection across western New York during the period of high winds. Farther aloft at 500 mb, a deep, meridional trough accompanied by a strong cyclonic vorticity center crosses western New York at about the time of high winds. The combination of strong anticyclonic vorticity advection coupled with strong cold air advection matches well with the Kapela et al. (1995) description of post cold frontal high wind events in the Northern Plains.

Composite atmospheric soundings for high wind events reveal surface to 850 mb lapse rates of about $8\,^{\circ}$C and little change in wind direction with height. In comparison, non high wind events that exhibited strong winds aloft had much weaker lapse rates and veering winds with height suggesting a subsidence inversion that prohibited downward momentum transfer and stronger winds to the surface.

Case studies of two events revealed additional information beyond the scope of climatological data. In addition to tightly packed surface isobars, high wind events were accompanied by very strong cold air advection through a deep layer of the atmosphere. The cold air advection led to strong subsidence and downward transport of higher momentum air across western New York as reflected in the advection of the 1000-500 mb thickness field. Both cases also revealed that high winds

occurred in conjunction with steep low level lapse rates that insured mixing of stronger winds aloft down to the surface. Finally, many of the processes conducive to high winds that occur higher in the atmosphere are reflected in one very important surface field, namely surface pressure rise/fall couplets that contribute to an isallobaric component of the wind. Both case studies revealed significant surface pressure rise/fall couplets that tracked along the direction of the prevailing wind in roughly a southwest to northeast direction.

This study serves to develop a climatology of non-convective high wind events in western New York. Composite synoptic scale patterns constructed from a twenty year data set of high wind events provide a general picture of the large scale weather patterns conducive to such events. Finally, select case studies highlight the most important forecast parameters as well as realtime surface data that can be utilized for the prediction of high wind events. The information provided here will hopefully serve as a reference for the operational forecaster in the prediction of non-convective high winds in western New York.

ACKNOWLEDGMENTS

REFERENCES

Angel, J.A., and Isard, S.A., 1998: The Frequency and Intensity of Great Lakes Cyclones. *Wea. Forecasting*, 11, 61-71.

Bluestein, H.B., 1992: Synoptic-Dynamic Meteorology in Midlatitudes. Oxford University Press, 594 pp.

Hubert, W.E., and Morford, D. 1987: Great Lakes Forecaster's Handbook, Jet Propulsion Laboratory Contract No. 957762, Ocean Data Systems, Monterey, CA 93490.

Kapela, A.F., Leftwich, P.W., Van Ess, R., 1995: Forecasting the Impacts of Strong Wintertime Post-Cold Front Winds in the northern Plains. *Wea. Forecasting*, 10, 229-244.

Lee, J.E. and Girodo, M., 1997: Use of the Eta model to Determine the Role of Static Stability in Forecasting Surface Winds. *Preprints, 16th Conf. On Weather Analysis and Forecasting,* Phoenix, AZ, Amer. Meteor. Soc., 56-58.

National Climatic Data Center, 1993: Solar and Meteorological Surface Observation Network 1961-1990, Volume 1.0, September, 1993. U.S. Department of Commerce.

National Climatic Data Center, 1985: Storm Data., Volume 27, No. 12, December 1985. U.S. Department of Commerce.

National Climatic Data Center, 1997: Storm Data., Volume 39, No. 02, February 1997. U.S. Department of Commerce.

National Climatic Data Center, 1995: Radiosonde data of North America 1946-1995. Version 1.8, August 1996 (Updated). U.S. Department of Commerce.

NCAR, 1990: National Meteorological Center Grid Point Data Set, Version III. Department of Atmospheric Sciences, University of Washington and the Data Support Section, National Center for Atmospheric Research, CD-ROM. [Available from National Center for Atmospheric Research, P.O. Box 3000, Boulder, CO 80307.]

Pore, A.N., Perrotti, H.P., Richardson, W.S., Climatology of Lake Erie Storm Surges at Buffalo and Toledo. NOAA Technical Memorandum NWS TDL-54, Silver Spring, MD, March 1975.

Richards, T.L., Dragert, H., McIntyre, D.R., 1966: Influence of Atmospheric Stability and Over-Water fetch on Winds Over the Lower Great Lakes. *Mon. Wea. Rev.*, 94, 448-453.

Saucier, W.J., 1955: Principals of Meteorological Analysis. The University of Chicago Press. 355 pp.

Table 1.   Top ten windiest cities in the continental U.S. during the period that extends from November through April (NCDC, CD-ROM Series).

Top Ten Windiest U.S. Cities During November Through April Time Frame

1. Blue Hill, MA   **17.0 mph**

2. Casper, WY   **14.7**

3. Cheyenne, WY   **14.5**

4. Dodge City, KS   **14.3**

5. Great Falls, MT   **14.2**

6. Rochester, MN   **14.1**

7. Amarillo, TX   **13.8**

8. Boston, MA   **13.5**

9. New York, NY (Laguardia)   **13.5**

10. Buffalo, NY   **13.2**

...

23. Erie, PA   **12.5**

...

33. Cleveland, OH   **11.9**

Table 2.   Temperature and wind data averaged for 52 high wind events and 132 "decoupled" non-high wind events during 1977-97 at Buffalo, NY.

Parameters	Events	Non- Events
Surface Temp (°C)	2.8	7.1
Surface Wind Speed (kts)	27.4	14.0
Surface Wind Direction	243	195
850 mb Temp (°C)	-5.2	3.5
850 mb Wind Direction	246	233
850 mb Wind Speed	53	57
Surface - 850 mb Temp (°C)	8.0	3.6
700 mb Temp (°C)	-11.7	-3.5
700 mb Wind Direction	253	240
700 mb Wind Speed	56	55

Table 3.   Temperature (°C), surface pressure, pressure tendencies at 1, 3 and 6 hours, and wind speed and direction at Buffalo, NY during 22 February 1997.

Time (UTC)	Temp (°C)	Pressure (mb)	delP (1hr / 3hr /6hr)	Wind
0500	12	993	- / - / -	SW 10
0600	15	993	0 / 0 / -	SW 22 G 29
0700	15	992	-1 / - / -	SW 17 G 25
0800	15	991	-1 / -2 / -	SW 22
0900	15	989	-2 / -4 / -	SW 21 G 27
1000	10	992	3 / 0 / -	SW 22 G 31
1100	6	993	1 / 2 / 0	SW 16
1200	4	994	1 / 5 / 1	SW 26 G 36
1300	2	995	1 / 3 / 3	SW 24 G 47
1400	-1	999	4 / 6 / 8	SW 38 G56
1500	-2	1003	4 / 9 / 14	SW 30 G 50
1600	–3	1005	2 / 10 / 13	SW 36 G 53
1700	-3	1007	2 / 8 / 14	SW 30 G 41
1800	-3	1009	2 / 6 / 15	SW 28 G 38
1900	-3	1010	1 / 5 / 15	SW 32 G 41
2000	-3	1012	2 / 5 / 13	SW 29 G 35
2100	-3	1013	1 / 4 / 10	SW 21 G 32
2200	-3	1014	1 / 4 / 9	SW 20
2300	-3	1014	0 / 2	SW 18 G 24
2400	-3	1016	2 / 3	SW 18 G 25

Table 4.   Temperature (°C), weather, surface pressure, pressure tendencies at 1, 3 and 6
hours, and wind speed and direction at Buffalo, NY during 27-28 February 1997.

Time (UTC)	Weather	Temp (°C)	Pressure (mb)	Del P 1 / 3 / 6hr	Winds
0500	R-	3	1003	- / - / -	NE 8
0600	R-	2	1002	-1 / - / -	NE 6
0700	R-	2	1002	0 / 0 / -	NE 6
0800	R	2	1002	0 / -1 / -	NE 5
0900	R	2	1000	-2 / -2 / -	ENE 7
1000	R	3	999	-1 / -3 / -	E 9
1100	R-	3	999	0 / -3 / -4	NE 6
1200	R-	3	997	-2 / -3 / -5	NE 12
1300	CY	3	996	-1 / -3 / -6	E 8
1400	R-	6	995	-1 / -4 / -7	SE 10
1500	R-	7	995	0 / -2 / -5	SE 9
1600	CY	11	993	-2 / -3 / -6	S 10
1700	PS	17	992	-1 / -3 / -7	SW 24 G 36
1800	PS	8	994	2 / -1 / -3	SW 23 G 31
1900	MS	7	996	2 / 3 / 0	SW 35 G 54
2000	MS	6	997	1 / 5 / 2	SW 36 G 56
2100	MC	6	999	2 / 5 / 4	SW 47 G 61
2200	CY	4	1001	2 / 5 / 8	SW 44 G 56
2300	CY	3	1004	3 / 7 / 12	SW 37 G 53
0000	CY	2	1007	3 / 8 / 13	SW 33 G 44
0100	CY	2	1010	3 / 9 / 14	SW 24 G 35
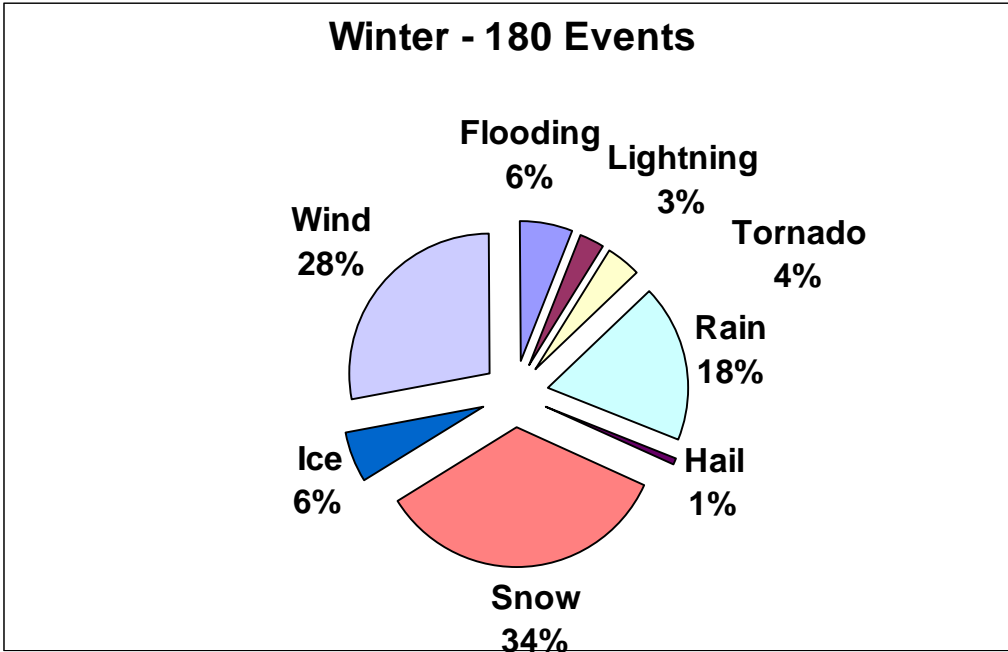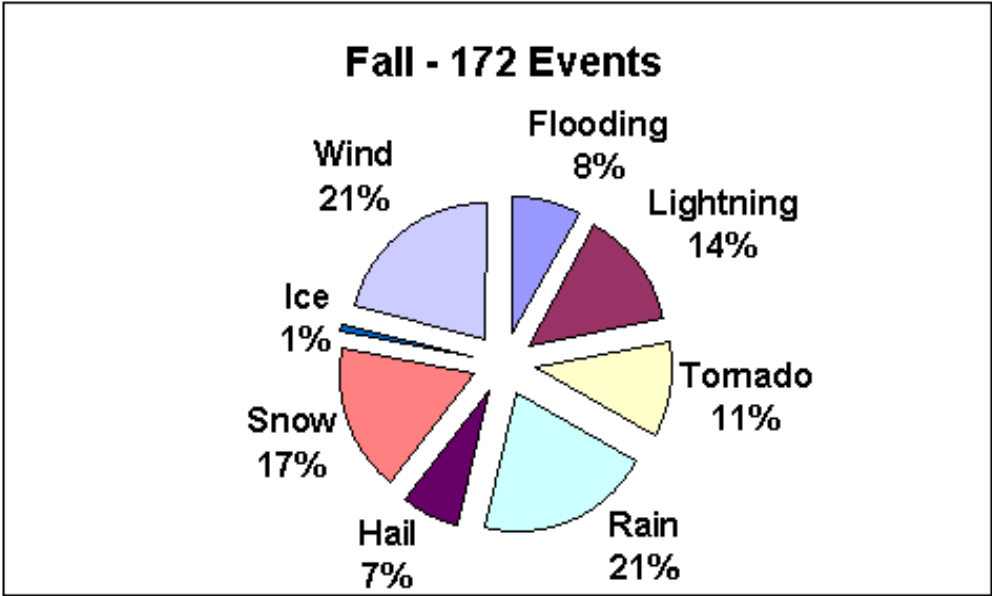
Figure 1.   Great Lakes Storm Climatology (1960-85) by weather element that caused at least one death or $500,000 damage to property and crops for Fall and Winter seasons across the Great Lakes Region (Hubert et al. 1987).

Seasonality of High Wind Events at Buffalo, NY
1977 - 1997
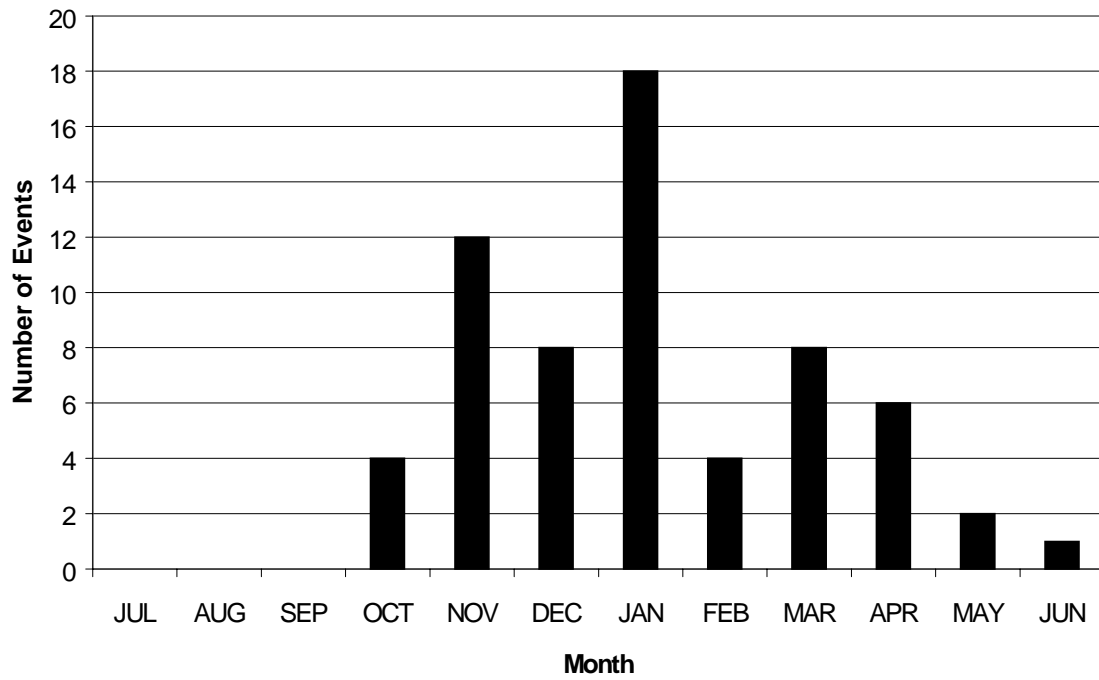
Figure 2.   High wind events for the time period 1977-97 at Buffalo, NY categorized by month.

Prevailing Wind Direction for Events at Buffalo, NY 1977-97
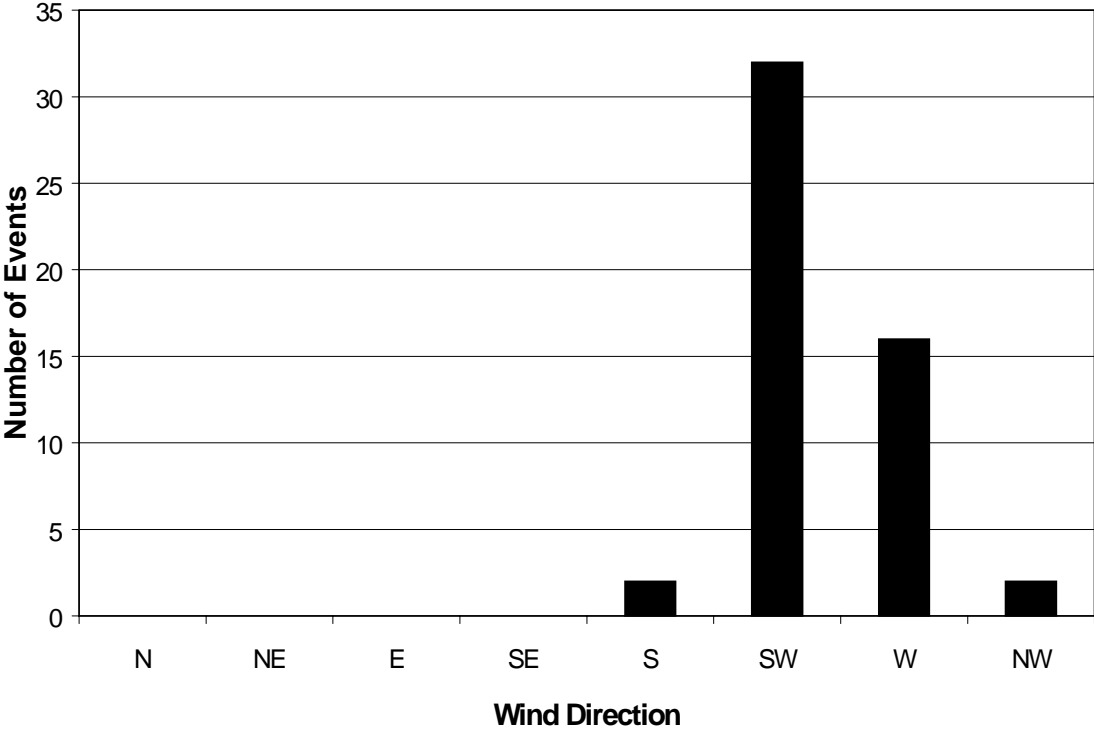
Figure 3.   The prevailing wind direction for high wind events at Buffalo, NY 1977-97.

October

November

December

January

February

March

April
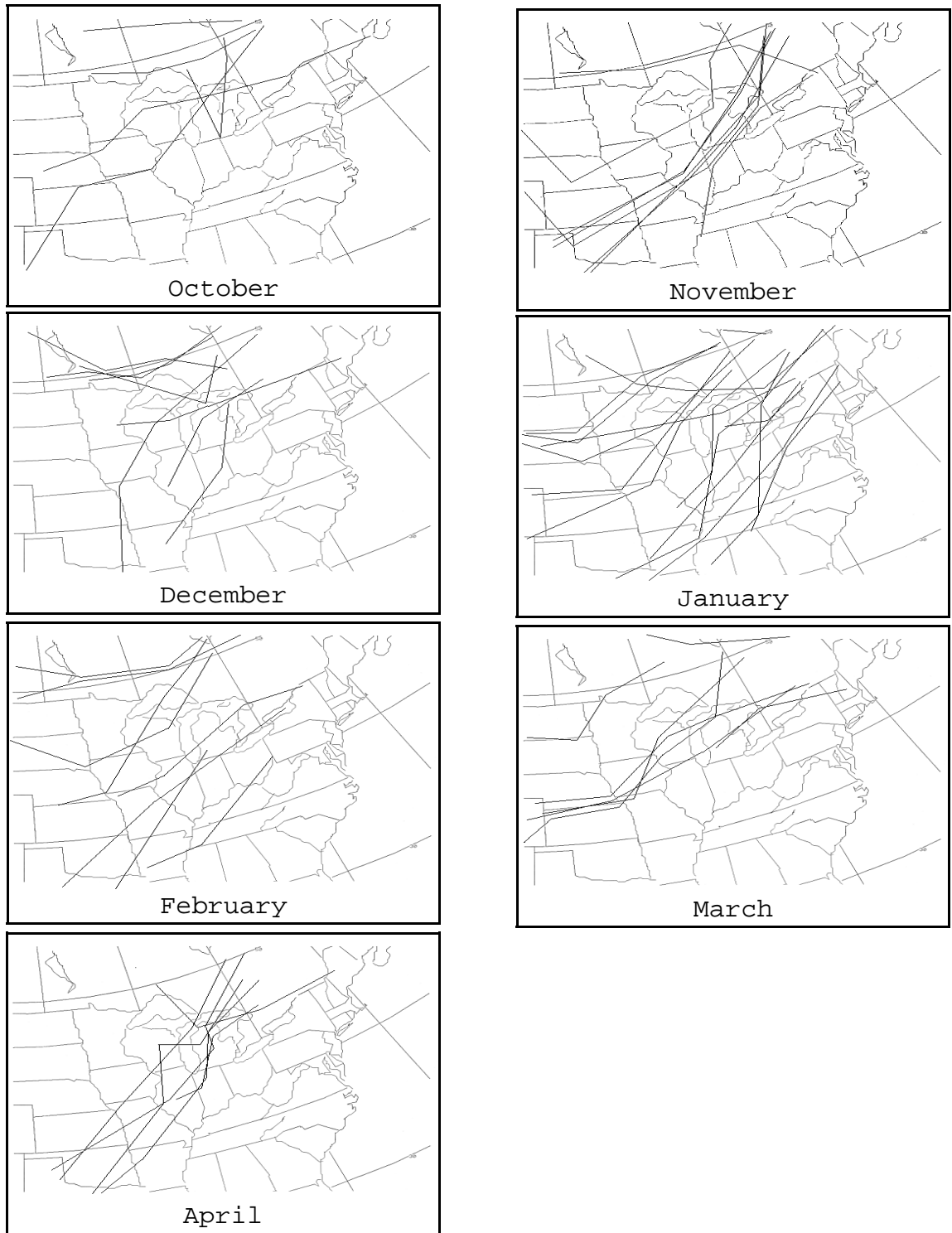
Figure 4.   Tracks of surface lows that produced high wind events in Buffalo, NY from 1977-97 during the late Fall through early Spring months.
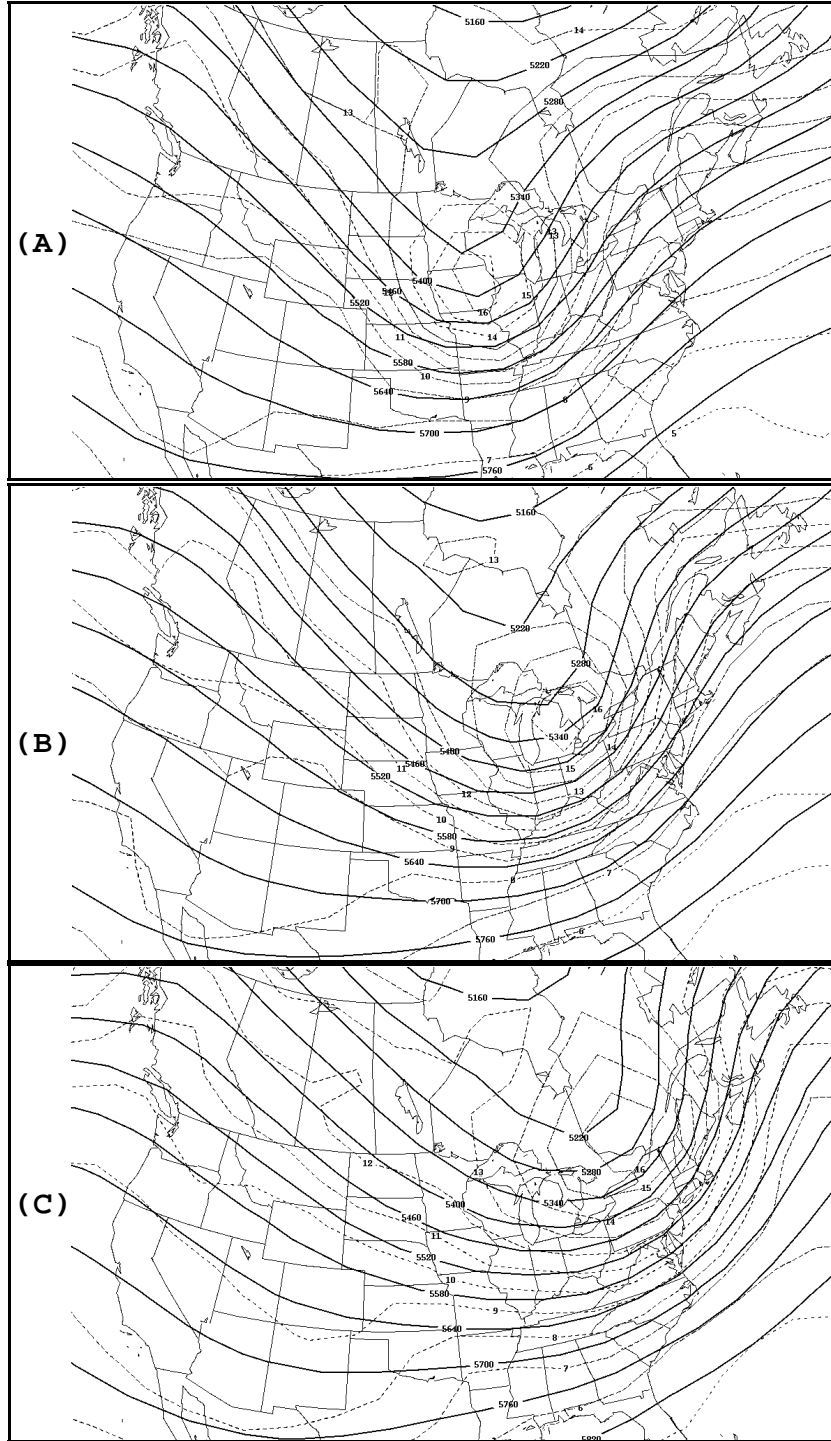
Figure 5. Composite charts of 500 mb geopotential height (dm) and vorticity for fifty-two high wind events at Buffalo, NY from 1977-97 for A). 12 hours before the event, B). About the time of the event and C). 12 hours after the event.

24
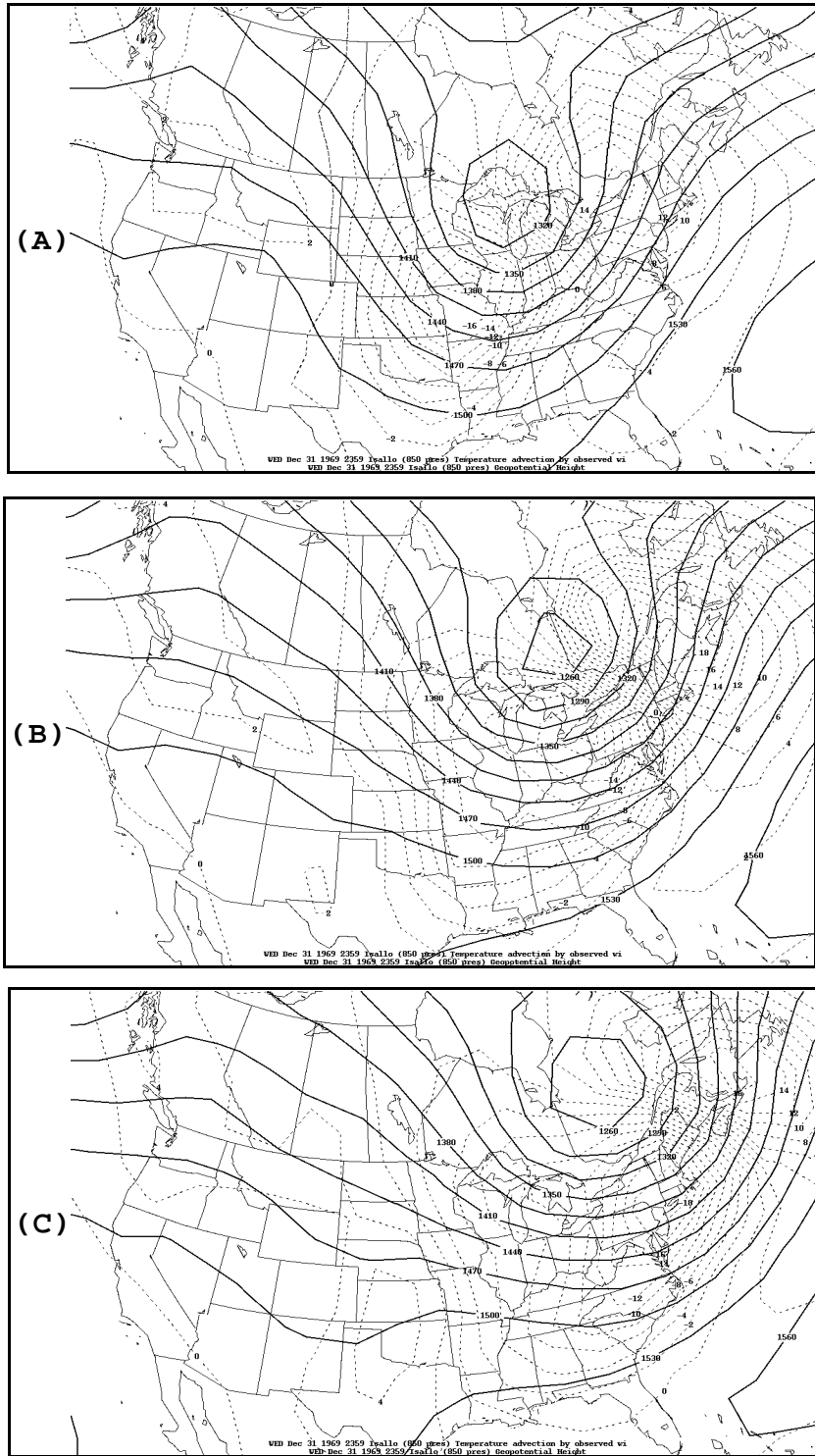
Figure 6.   Composite charts of 850 mb geopotential height (dm) and temperature advection for fifty-two high wind events at Buffalo, NY from 1977-97 for A). 12 hours before the event, B). About the time of the event and C). 12 hours after the event.
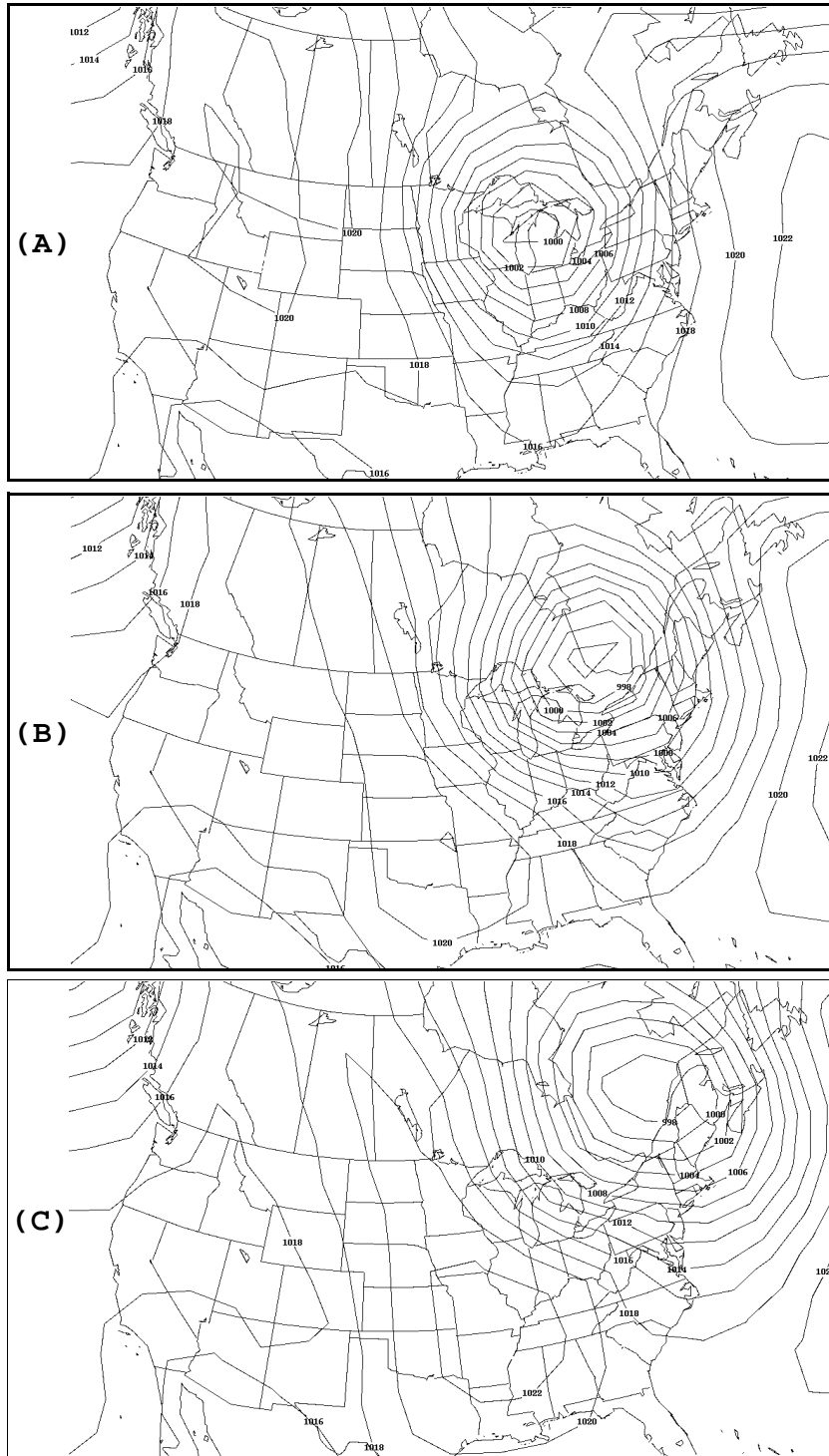
Figure 7. Composite charts of Mean Sea Level Pressure (mb) for fifty-two high wind events at Buffalo, NY from 1977-97 for A). 12 hours before the event, B). About the time of the event and C). 12 hours after the event
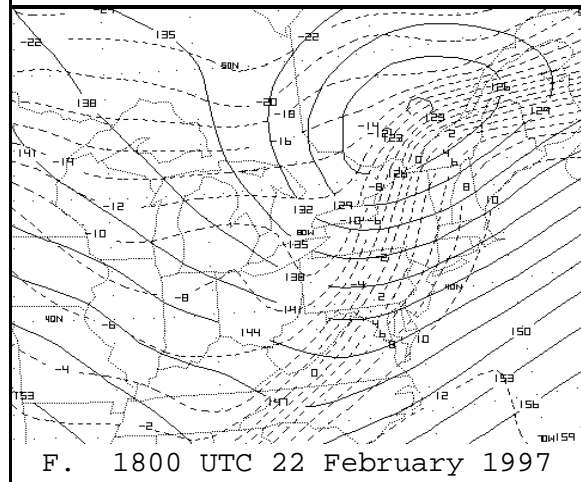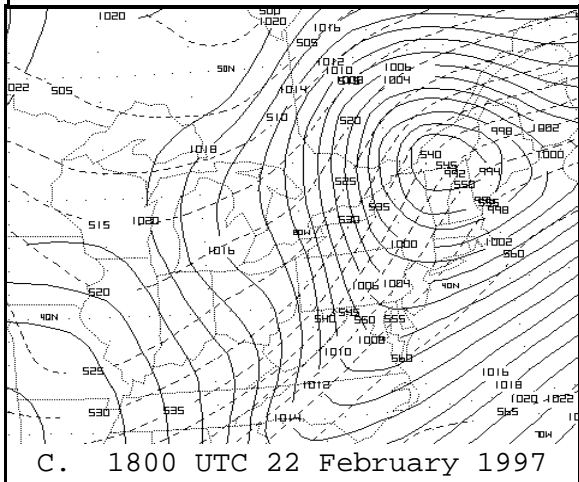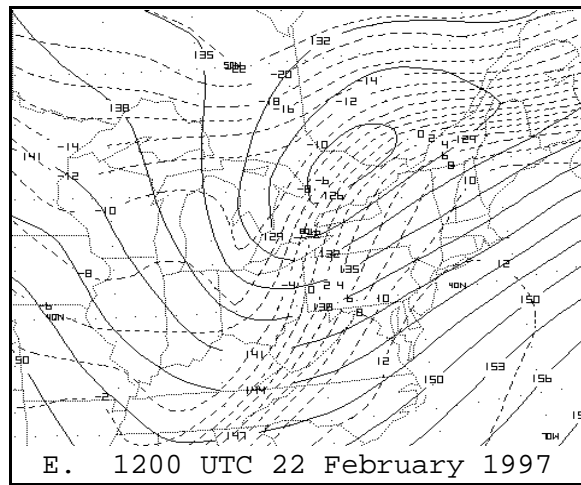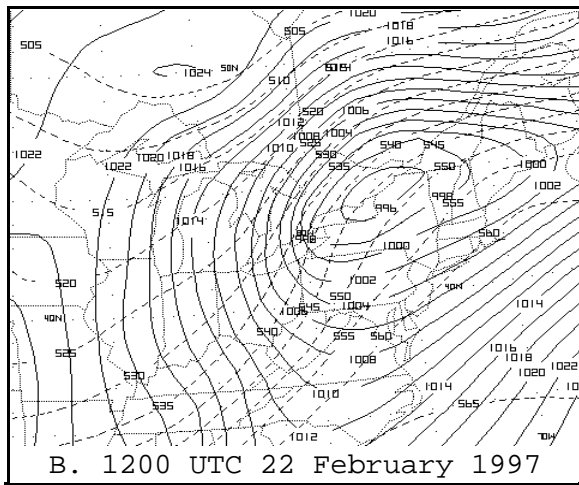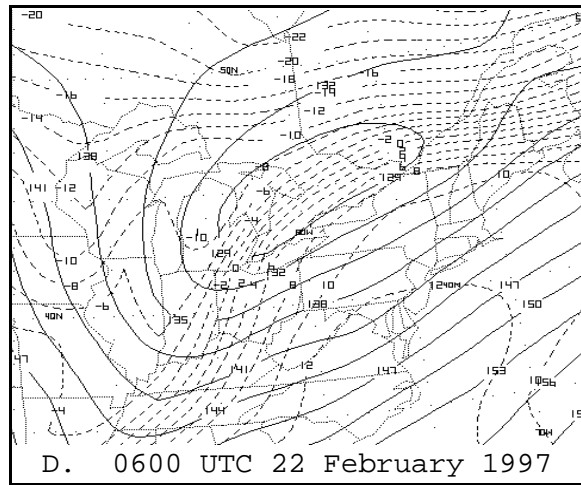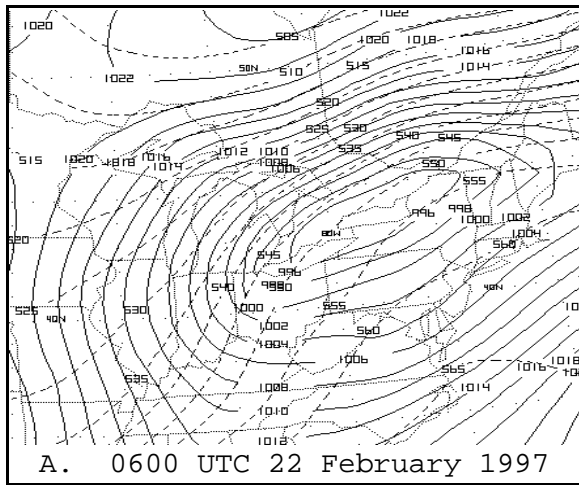
Figure 8. 0000 UTC 22 February 1997 Eta forecast at 06, 12 and 18hrs for: a-c) mean sea level pressure (solid lines) and 1000-500 mb thickness (dashed) and d-f) 850 mb height (solid lines) and temperature (dashed).
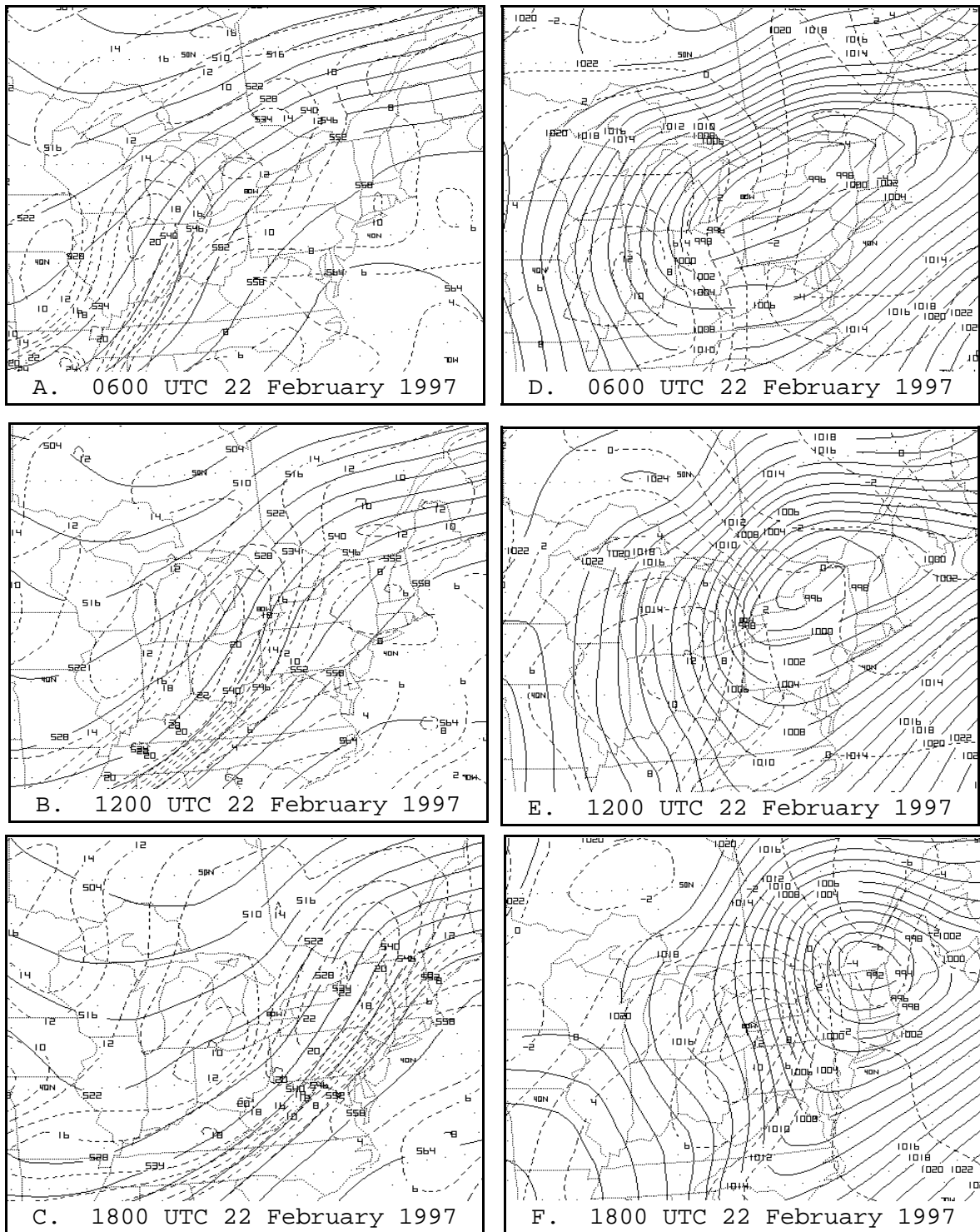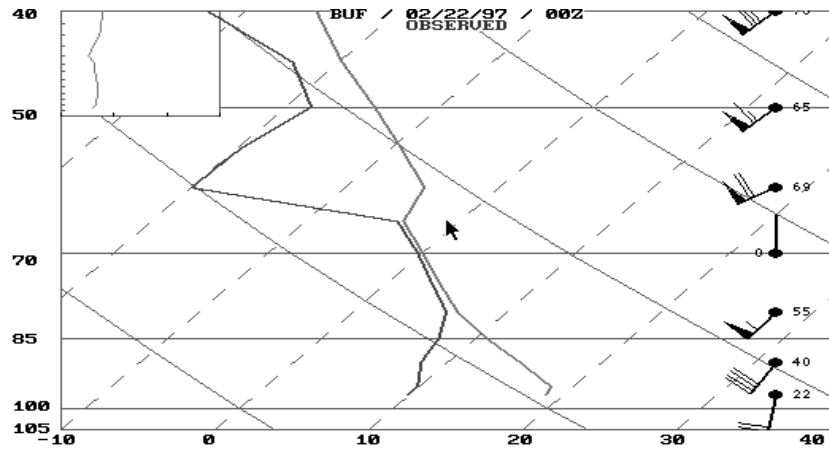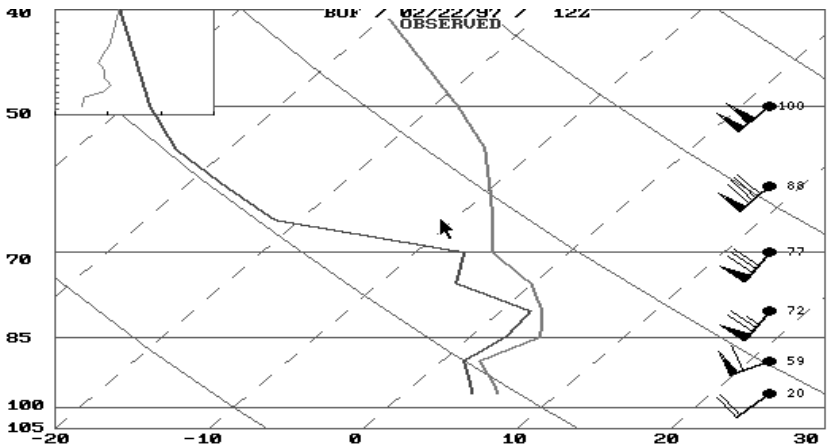
A.   0600 UTC 22 February 1997

D.   0600 UTC 22 February 1997

B.   1200 UTC 22 February 1997

E.   1200 UTC 22 February 1997

C.   1800 UTC 22 February 1997

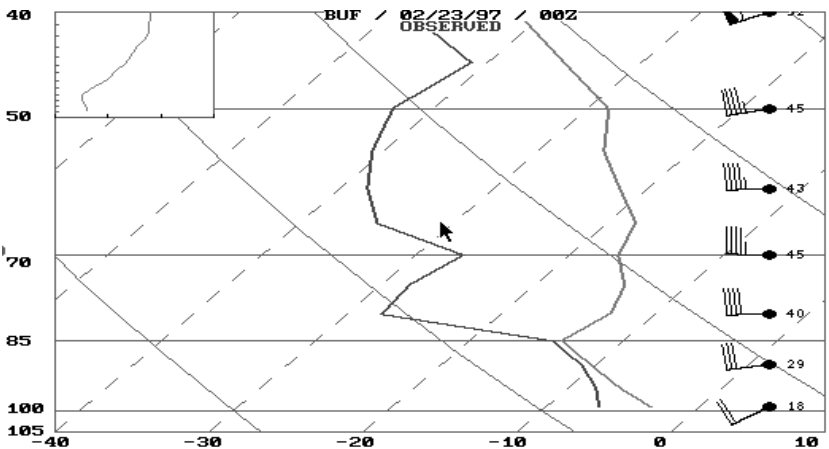F.   1800 UTC 22 February 1997

Figure 9.   0000 UTC 22 February 1997 Eta forecast at 06, 12 and 18hrs for: a-c) 1000/500 mb thickness (solid lines) and 500 mb vorticity (dashed), and d-f) mean sea level pressure (solid lines) and 6 hr surface pressure change (dashed).

Figure 10. Observed soundings at Buffalo, NY taken at a). 0000 UTC 22 February 1997, b).
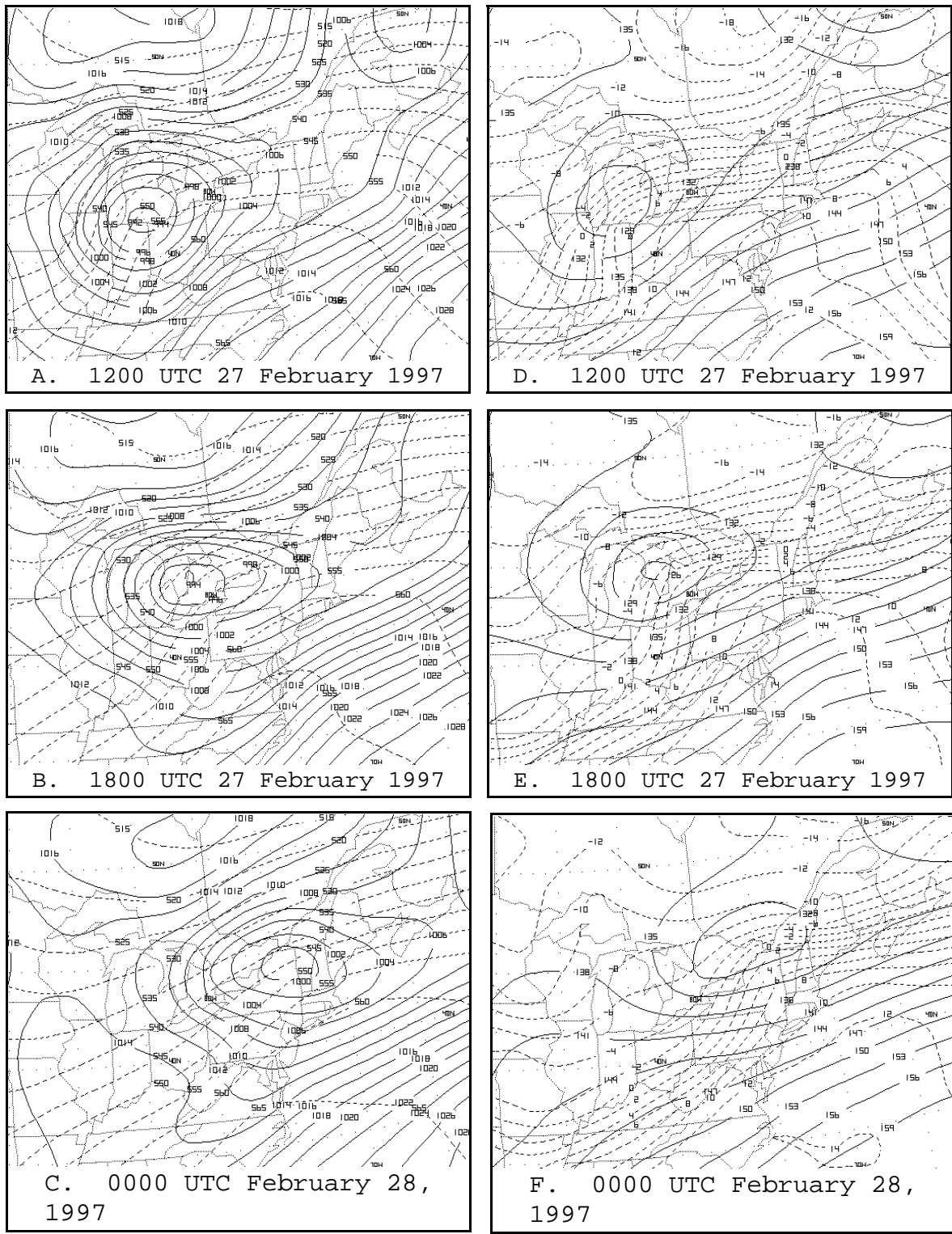   1200 UTC 22 February 1997, and c). 0000 UTC 23 February 1997.

Figure 11. 1200 UTC 27 February 1997 Eta forecast at 06, 12 and 18hrs for: a-c) 1000/500 mb thickness (solid lines) and 500 mb vorticity (dashed), and d-f) mean sea level pressure (solid lines) and 6 hr surface pressure change (dashed).

A.   1200 UTC 27 February 1997
D.   1200 UTC 27 February 1997
B.   1800 UTC 27 February 1997
E.   1800 UTC 27 February 1997
C.   0000 UTC 28 February 1997
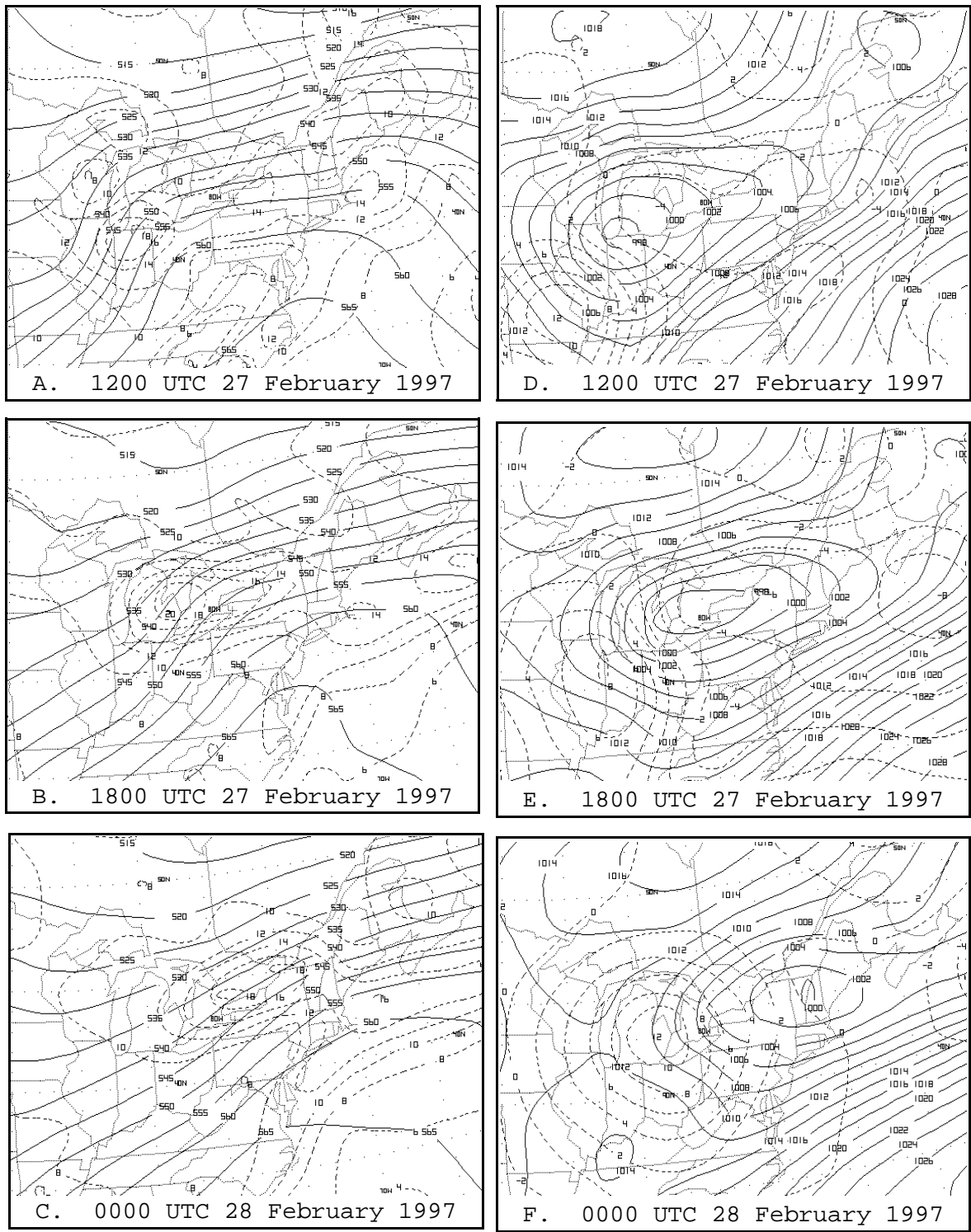F.   0000 UTC 28 February 1997

Figure 12. 1200 UTC 27 February 1997 Eta forecast at 00, 06 and 12hrs for: a-c) 1000/500 mb thickness (solid lines) and 500 mb vorticity (dashed), and d-f) mean sea level pressure (solid lines) and 6 hr surface pressure change (dashed).
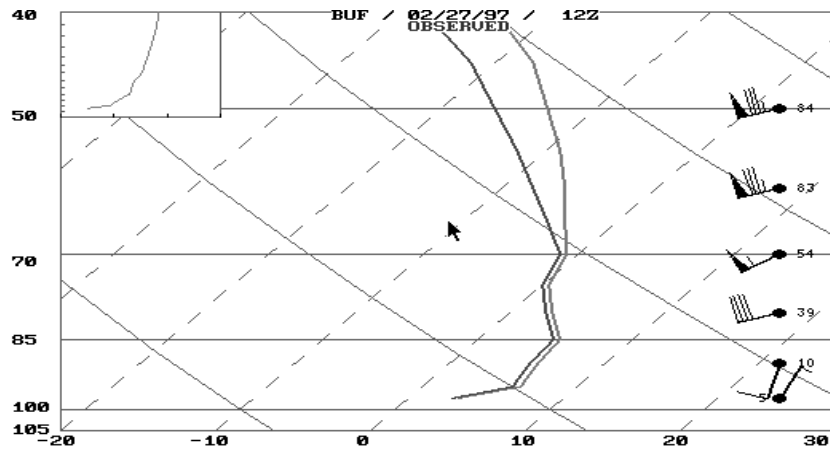
Figure 13. Observed sounding at Buffalo, NY taken at a). 1200 UTC 27 February 1997
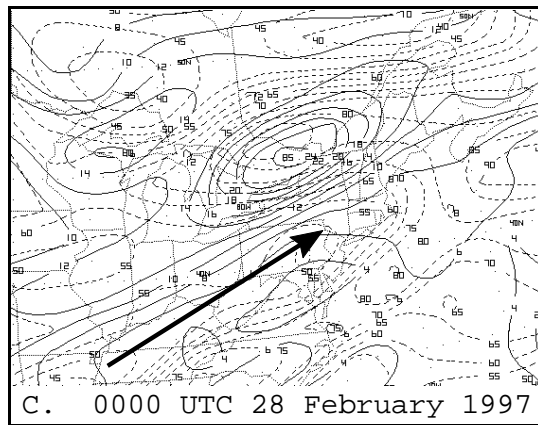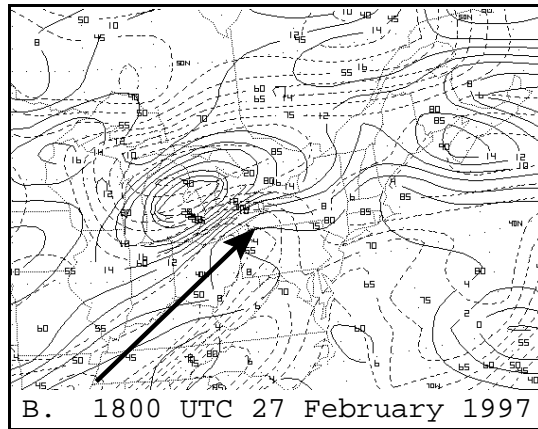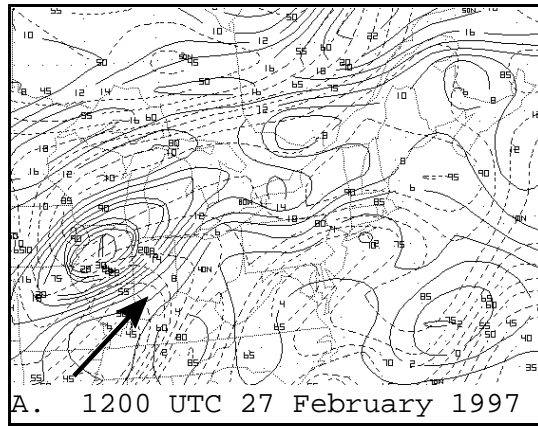
Figure 14. 1200 UTC 27 February 1997 Eta model forecast at 00, 06 and 12hrs for 500mb
vorticity (solid lines) and 1000/500 mb relative humidity (dashed). Heavy Solid
arrows show the location of the dry slot.

NWS ER 46 An Objective Method of Forecasting Summertime Thunderstorms. John F. Townsend and Russell J. Younkin. May 1972. (COM-72-10765).
NWS ER 47 An Objective Method of Preparing Cloud Cover Forecasts. James R. Sims. August 1972. (COM-72-11382).
NWS ER 48 Accuracy of Automated Temperature Forecasts for Philadelphia as Related to Sky Condition and Wind Direction. Robert B. Wassall. September 1972. (COM-72-11473).
NWS ER 49 A Procedure for Improving National Meteorological Center Objective Precipitation Forecasts. Joseph A. Ronco, Jr. November 1972. (COM-73-10132).
NWS ER 50 PEATMOS Probability of Precipitation Forecasts as an Aid in Predicting Precipitation Amounts. Stanley E. Wasserman. December 1972. (COM-73-10243).
NWS ER 51 Frequency and Intensity of Freezing Rain/Drizzle in Ohio. Marvin E. Miller. February 1973. (COM-73-10570).
NWS ER 52 Forecast and Warning Utilization of Radar Remote Facsimile Data. Robert E. Hamilton. July 1973. (COM-73-11275).
NWS ER 53 Summary of 1969 and 1970 Public Severe Thunderstorm and Tornado Watches Within the National Weather Service, Eastern Region. Marvin E. Miller and Lewis H. Ramey. October 1973. (COM-74-10160)
NWS ER 54 A Procedure for Improving National Meteorological Center Objective Precipitation Forecasts - Winter Season. Joseph A. Ronco, Jr. November 1973. (COM-74-10200).
NWS ER 55 Cause and Prediction of Beach Erosion. Stanley E. Wasserman and David B. Gilhousen. December 1973.(COM-74-10036).
NWS ER 56 Biometeorological Factors Affecting the Development and Spread of Planet Diseases. V.J. Valli. July 1974. (COM-74-11625/AS).
NWS ER 57 Heavy Fall and Winter Rain In The Carolina Mountains. David B. Gilhousen. October 1974. (COM-74-11761/AS).
NWS ER 58 An Analysis of Forecasters' Propensities In Maximum/Minimum Temperature Forecasts. I. Randy Racer. November 1974. COM-75-10063/AS.
NWS ER 59 Digital Radar Data and its Application in Flash Flood Potential. David D. Sisk. March 1975. (COM-75-10582/AS).
NWS ER 60 Use of Radar Information in Determining Flash Flood Potential. Stanley E. Wasserman. December 1975. (PB250071/AS).
NWS ER 61 Improving Short-Range Precipitation Guidance During the Summer Months. David B. Gilhousen. March 1976. (PB256427).
NWS ER 62 Locally Heavy Snow Downwind from Cooling Towers. Reese E. Otts. December 1976. (PB263390/AS).
NWS ER 63 Snow in West Virginia. Marvin E. Miller. January 1977. (PB265419/AS).
NWS ER 64 Wind Forecasting for the Monongahela National Forest. Donald E. Risher. August 1977. (PB272138/AS).
NWS ER 65 A Procedure for Spraying Spruce Budworms in Maine during Stable Wind Conditions. Monte Glovinsky. May 1980. (PB80-203243).
NWS ER 66 Contributing Factors to the 1980-81 Water Supply Drought, Northeast U.S. Solomon G. Summer. June 1981. (PB82-172974).
NWS ER 67 A Computer Calculation and Display System for SLOSH Hurricane Surge Model Data. John F. Townsend. May 1984. (PB84-198753).
NWS ER 68 A Comparison Among Various Thermodynamic Parameters for the Prediction of Convective Activity. Hugh M. Stone. April 1985. (PB85-206217/AS).
NWS ER 69 A Comparison Among Various Thermodynamic Parameters for the Prediction of Convective Activity, Part II. Hugh M. Stone. December 1985. (PB86-142353/AS).
NWS ER 70 Hurricane Gloria's Potential Storm Surge. Anthony G. Gigi and David A. Wert. July 1986. (PB86-226644/AS).
NWS ER 71 Washington Metropolitan Wind Study 1981-1986. Clarence Burke, Jr. and Carl C. Ewald. February 1987. (PB87-151908/AS).
NWS ER 72 Mesoscale Forecasting Topics. Hugh M. Stone. March 1987. (PB87-180246/AS).
NWS ER 73 A Procedure for Improving First Period Model Output Statistics Precipitation Forecasts. Antonio J. Lacroix and Joseph A. Ronco. Jr. April 1987. (PB87-180238/AS).
NWS ER 74 The Climatology of Lake Erie's South Shoreline. John Kwiatkowski. June 1987. (PB87-205514/AS).
NWS ER 75 Wind Shear as a Predictor of Severe Weather for the Eastern United States. Hugh M. Stone. January 1988. (PB88-157144).
NWS ER 76 Is There A Temperature Relationship Between Autumn and the Following Winter? Anthony Gigi. February 1988. (PB88-173224).
NWS ER 77 River Stage Data for South Carolina. Clara Cillentine. April 1988. (PB88-201991/AS).
NWS ER 78 National Weather Service Philadelphia Forecast Office 1987 NOAA Weather Radio Survey & Questionnaire. Robert P. Wanton. October 1988. (PB89-111785/AS).
NWS ER 79 An Examination of NGM Low Level Temperature. Joseph A. Ronco, Jr. November 1988. (PB89- 122543/AS).
NWS ER 80 Relationship of Wind Shear, Buoyancy, and Radar Tops to Severe Weather 1988. Hugh M. Stone. November 1988. (PB89-1222419/AS).
NWS ER 81 Relation of Wind Field and Buoyancy to Rainfall Inferred from Radar. Hugh M. Stone. April 1989. (PB89-208326/AS).
NWS ER 82 Second National Winter Weather Workshop, 26-30 Sept. 1988: Postprints. Laurence G. Lee. June 1989.(PB90-147414/AS).
NWS ER 83 A Historical Account of Tropical Cyclones that Have Impacted North Carolina Since 1586. James D. Stevenson. July 1990. (PB90-259201).
NWS ER 84 A Seasonal Analysis of the Performance of the Probability of Precipitation Type Guidance System. George J. Maglaras and Barry S. Goldsmith. September 1990. (PB93-160802)
NWS ER 85 The Use of ADAP to Examine Warm and Quasi-Stationary Frontal Events in the Northeastern United States. David R. Vallee. July 1991. (PB91-225037)
NWS ER 86 Rhode Island Hurricanes and Tropical Storms A Fifty-Six Year Summary 1936-0991. David R. Vallee. March 1993. (PB93-162006)
NWS ER 87 Post-print Volume, Third National Heavy Precipitation Workshop, 16-20 Nov. 1992. April 1993. (PB93-186625)
NWS ER 88 A Synoptic and Mesoscale Examination of the Northern New England Winter Storm of 29-30 January 1990. Robert A. Marine and Steven J. Capriola. July 1994. (PB94-209426)
NWS ER 89 An Initial Comparison of Manual and Automated Surface Observing System Observations at the Atlantic City, New Jersey, International Airport. James C. Hayes and Stephan C. Kuhl. January 1995 (PB95-213492)
NWS ER 90 Numerical Simulation Studies of the Mesoscale Environment Conducive to the Raleigh Tornado. Michael L. Kaplan, Robert A. Rozumalski, Ronald P. Weglarz, Yuh-Lang Lin , Steven Businger, and Rodney F. Gonski. November 1995.

NOAA SCIENTIFIC AND TECHNICAL PUBLICATIONS

The National Oceanic and Atmospheric Administration was established as part of the Department of Commerce on October 3, 1970. The mission responsibilities of NOAA are to assess the socioeconomic impact of natural and technological changes in the environment and to monitor and predict the state of the solid Earth, the oceans and their living resources, the atmosphere, and the space environment of the Earth.

The major components of NOAA regularly produce various types of scientific and technical information in the following kinds of publications:

PROFESSIONAL PAPERS--Important definitive research results, major techniques, and special investigations.

CONTRACT AND GRANT REPORTS--Reports prepared by contractors or grantees under NOAA sponsorship.

ATLAS--Presentation of analyzed data generally in the form of maps showing distribution of rainfall, chemical and physical conditions of oceans and atmosphere, distribution of fishes and marine mammals, ionospheric conditions, etc.

TECHNICAL SERVICE PUBLICATIONS--Reports containing data, observations, instructions, etc. A partial listing includes data serials; prediction and outlook periodicals; technical manuals, training papers, planning reports, and information serials; and miscellaneous technical publications.

TECHNICAL REPORTS--Journal quality with extensive details, mathematical developments, or data listings.

TECHNICAL MEMORANDUMS--Reports of preliminary, partial, or negative research or technology results, interim instructions, and the like.

Information on availability of NOAA publications can be obtained from:

NATIONAL TECHNICAL INFORMATION SERVICE
U.S. DEPARTMENT OF COMMERCE
5285 PORT ROYAL ROAD
SPRINGFIELD, VA 22161